VYSOKÉ UČENÍ TECHNICKÉ V BRNĚ

BRNO UNIVERSITY OF TECHNOLOGY

FAKULTA ELEKTROTECHNIKY A KOMUNIKAČNÍCH TECHNOLOGIÍ

ÚSTAV RADIOELEKTRONIKY

FACULTY OF ELECTRICAL ENGINEERING AND COMMUNICATION
DEPARTMENT OF RADIO ELECTRONIC

NUMERICAL SYNTHESIS OF FILTERING ANTENNAS

NUMERICKÁ SYNTÉZA FILTRUJÍCÍCH ANTÉN

SHORT VERSION OF DOCTORAL THESIS

ZKRÁCENÁ VERZE DOKTORSKÉ PRÁCE

AUTHOR — Ing. MARTIN KUFA

AUTOR PRÁCE

SUPERVISOR — Prof. ZBYNĚK RAIDA

VEDOUCÍ PRÁCE

BRNO 2015

KEYWORDS

Filtering antenna array; filtenna; band-pass filter; low-pass prototype filter; low-pass transformation; g_i coefficients; normalized realized gain.

KLÍČOVÁ SLOVA

Filtrující anténní řada; filténa; filtr typu pásmová propust; prototypový filtr typu dolní propust; transformace na filtr typu dolní propust; g_i koeficienty; normovaný realizovaný zisk.

STORAGE PLACE

Research department, FEEC BUT, Technická 3058/10, 602 00 Brno

MÍSTO ULOŽENÍ PRÁCE

Vědecké oddělení, FEKT VUT v Brně, Technická 3058/10, 602 00 Brno

ACKNOWLEDGEMENT

The research described in my thesis was performed in laboratories of the SIX Research Center, the registration number CZ.1.05/2.1.00/03.0072, the operational program Research and Development for Innovation.

CONTENTS

1 INTRODUCTION

Nowadays, wireless devices play an increasingly important role. We use such devices in daily life almost continuously. In future, more and more new devices will use wireless connections. With the proliferation of new devices, we start to face two problems. First, existing frequency bands are overcrowded, and therefore, higher and higher frequency bands have to be used (that way, the growing demands on the transmission speed and the amount of data transferred can be met also). Second, flexibility and mobility of wireless devices have to be improved.

In order to minimize dimensions of mobile devices, we can implement fractal theory to the design of an antenna. The fractal design can also reduce the size of filters. Further reduction of the filter size can be achieved by using the concept of defected ground structures. Finally, an antenna and a filter can be integrated into a single, compact structure of minimal dimensions.

The combination of an antenna and a filter into a single, compact structure is called filtering antenna or filtenna. A simultaneous frequency and space filtering is the main task of the filtenna. In an ideal case, a band-pass filter does not need to be used on the receiving side because the filtering is done by the filtenna.

In this report, we discuss the methodology of the design of filtering antennas which do not contain filter elements. Filtering abilities are here achieved by suitably designed structure of an antenna array.

In Chapter 2, we analyze state of the art of the synthesis of filtering antennas. Different approaches are mutually compared, and problems to be solved are identified. Considering results of the analysis, we define objectives of the dissertation in Chapter 3. In Chapters 4, planar filtering antenna array fed by apertures is presented and its equivalent circuit and low-pass transformation are described in Chapter 5. Chapter 6 is focused on the complete synthesis approach of the filtering antenna array and in the Chapter 7, the confrontation of the simulated and measured results of the filtennas are mentioned. Chapter 8 concludes the report.

2 STATE OF THE ART

This Section reviews recent developments in the field of filtering antennas (filtennas). We will concentrate on three main approaches to the design of filtennas:

- A separate planar filter and a separate planar antenna are integrated. As a planar filter, a microstrip band-pass filter or a SIW (substrate integrated waveguide) band-pass filter are used. As a planar antenna, a patch antenna or a patch array are exploited.
- In the structure of a planar filter, the last resonator of a filter is replaced by a patch antenna or a monopole. Such a structure can be designed by a filter synthesis approach.
- The filtering antenna (the filtenna) is created only by radiating elements without any filtering parts. The frequency response of the realized gain is synthesized by optimization of all radiating elements, distances of the neighboring elements and amplitude and phase excitations of each individual element.

The following Chapters describe the methods in detail.

2.1 Combination of band-pass filter and antenna

The first part of the filtering antenna is created by a band-pass filter and the second one is formed by any radiating element. In [1], authors have described a third-order SIW inductive window filter which is coupled with a slot antenna or two-slot antenna array. In [2], a five-cavity SIW filter was connected with a six-element printed Yagi antenna. A structure consisting of a third-order cavity window band-pass filter integrated into SIW and a planar coaxial collinear (COCO) radiation element was described in [3]. A tunable filtennas using a band-pass filter with a varactor and a wideband dual-side Vivaldi antenna were discussed in [4], [5] and [6]. In [7], authors combine two third-order stopband filters with binomical balun and single dipole antenna. In these cases, filters and antennas or antenna arrays are designed absolutely separately on one common substrate.

2.2 Integration of radiating element into filter

Several papers describe a design of filtennas using a filter synthesis approach. Filtennas consist of a band-pass filter with an integrated radiating element as a last resonator of the filter. In this case, the filtenna is designed as complete device, but filtering and radiating parts can be clearly identified.

A last open-loop resonator and an output port of three microstrip square open-loops filter were replaced by a coupled line and a Γ-shaped antenna [8] or by center fed circular patch antenna and a coupled annular ring [9]. The coupled line was used as an admittance inverter.

In [10], authors presented a microstrip patch antenna integrated into a three-pole hairpin band-pass filter. In [10], an equivalent circuit including a patch and filter approach for design of the filtenna was designed.

In [11], a filtering microstrip *U*-shaped antenna with a *T*-shaped resonator in a feeder which operates together as a second-order quasi-elliptic band-pass filter with two zeroes at the band edges was published. The design of a filtering microstrip antenna array based on [11] was described in [12] and [13].

A printed meander-line antenna with quarter-wavelength resonator filter which operate together as the second-order filtenna was published in [14]. The described issue was followed in [15] and [16]. The design procedure was identical with [14] but the meander-line antenna was replaced by the *Γ*-shaped antenna and the quarter-wavelength resonator was replaced by a defected ground plane (DGS) resonator. A similar design of a filtering antenna was presented in [17]. The filtering antenna was created by an inverted *L*-shaped antenna and a quarter-wavelength resonator.

In [18], authors designed a filtering antenna which was composed by a parallel coupled microstrip line band-pass filter and an inverted *L*-shaped antenna.

A low-pass filter with reduced fractal defected ground structure (DGS) [19]–[21] can be used as a basic element to design of a filtenna [22]. This filter exhibits two passband ranges and owing to the addition of three capacitive elements and removed the second output port, the filter behaves like the filtenna at the second operating band [22].

2.3 Filtering antennas with synthesized realized gain

The last main approach to the design of filtennas is based on the antenna array, where the frequency response of the realized gain is synthesized by optimization of the dimensions, amplitude and phase excitations and distances between neighboring radiating elements. Due to described approach, authors could shape the frequency response of the realized gain and obtain the required response.

In [7], authors described the series fed patch antenna array consisting of five radiating elements. In the structure, each patch antenna and each transmission line have different dimensions, which were the subjects of the optimization process.

Another way to synthesis of the realized gain of the antenna array was presented in [7] and [23] as well. In this case, authors assumed an idealized antenna model without couplings between neighboring radiating elements. The idealized antenna array was optimized by particle swarm.

The synthesis of a dipole antenna array was described in [23] and [24]. In this case, authors used a multi-objectives self-organizing algorithm. Firstly, authors optimized the antenna array without any feeders among neighboring dipoles. Secondly, the feeders among the dipoles were considered to the model. Due to described models, authors could shape gain and level of side lobes and control the responses of the gain and the reflection coefficient.

3 DISSERTATION OBJECTIVES

In Chapter 2, the recent developments in the field of filtering antennas were presented. The analysis clearly identified new directions of the research in the field of filtering antennas:

- Methodologies for the design of filtering arrays without filter modules have not been published yet. The filtering array should be designed such a way so that the excitation current is reflected from the input port in the stop band or enters the antenna in the pass-band.
- Proper equivalent circuits of filtering antennas to be used for filtenna synthesis are missing. A design based on an equivalent circuit can significantly improve synthesis of filtennas.
- Synthesis approaches applying a band-pass filter design to the synthesis of filtering arrays have not been developed yet. A filter design procedure following the line from a low-pass prototype to a band-pass filter is attractive to be exploited for the design of filtennas.
- Methods of controlling the frequency response of the realized gain have not been satisfactorily described yet. In case of a filter, the output voltage is related to time derivatives of the input voltage. In case of a filtenna, the output gain is related to the integral of current distributions (amplitudes and phases) on the planar structure. Therefore, advanced techniques have to be developed to make frequency dependencies of gain sharper, and to suppress variations of the main-lobe direction.

Therefore, we can define the following objectives of the dissertation:

- A methodology of selecting an appropriate geometry of a filtering array will be worked out and verified.

  In the thesis, we will investigate various geometries of antenna arrays. The geometries will be evaluated from the viewpoint of resonances. A suitable antenna array should show a single resonance without parasitic ones in the operation band. In the frequency region of resonance, the filtering array should be matched (the excitation power passes from the feeder to the main lobe direction) and the main lobe direction should be stable. Applying optimization techniques, the width of the operation band should be maximized.

- We will develop methodology of synthesizing filtering antennas based on an equivalent circuit concept.

  An equivalent circuit of a single antenna element and the entire antenna array should be suitable for the application of the band-pass filter approach. In an ideal case, the equivalent circuit will consist of R, L and C lumped components, an impedance inverter or an admittance inverter only.

  The filtering antenna will be synthesized by using the band-pass filter approach. Starting from normalized values of a low-pass prototype filter, the band-pass filter can be designed. That way, an equivalent circuit of a filtenna is obtained. In the

final step, the equivalent circuit is converted to the geometry of the filtering antenna.

- Methods of stabilizing the direction and the shape of the main lobe in the operation band of the filtenna will be developed and verified.

  For space filtering, the direction of the main lobe should be perpendicular to the substrate with small variations. The frequency response of the realized gain is asked to behave like a transmission coefficient of a band-pass filter.

  Since the frequency response of the realized gain is related to the integral of current distributions on the filtenna layout, the requested stability of parameters has to be achieved by a proper feeding (a stable amplitude and phase of currents at elements within the operation band), or by compensation techniques (influences of feeding network and antenna elements should exhibit opposite effects.

In the following Chapter, so-far achievements are summarized.

4 PLANAR FILTERING ANTENNA ARRAY

In this Section, the selection of an appropriate structure of a filtering antenna array will be discussed. We will concentrate on a planar antenna array fed by apertures which is a good candidate for the implementation of filtering antennas. An influence of dimensions of an aperture and length of an open end on the mutual capacitance and coupling will be investigated. The influence of these parameters will be described by equations in order to easily implement these dependencies.

4.1 Comparison of properties of planar antenna arrays

When choosing a suitable configuration of an antenna array to be used for the design of the filtering array, following demands have to be considered:

- The antenna array should operate without parasitic resonances.
- The direction of the main lobe should not depend on the frequency and should be perpendicular to the antenna array (*z*-direction in Figure 4.1).
- The feeding network should not affect radiation patterns and the main lobe direction.

As a compromise, we can use the "out-of-line" serial feeding network of the antenna array [25]. In order to minimize the influence of the feeder on the radiation patters and the main lobe direction, the antenna array fed by apertures was selected for the final design of the filtering antenna array. Due to this solution, two substrates have to be used. Nevertheless, all the requirements are sufficiently met. The filtering antenna array fed by apertures is shown in Figure 4.1.

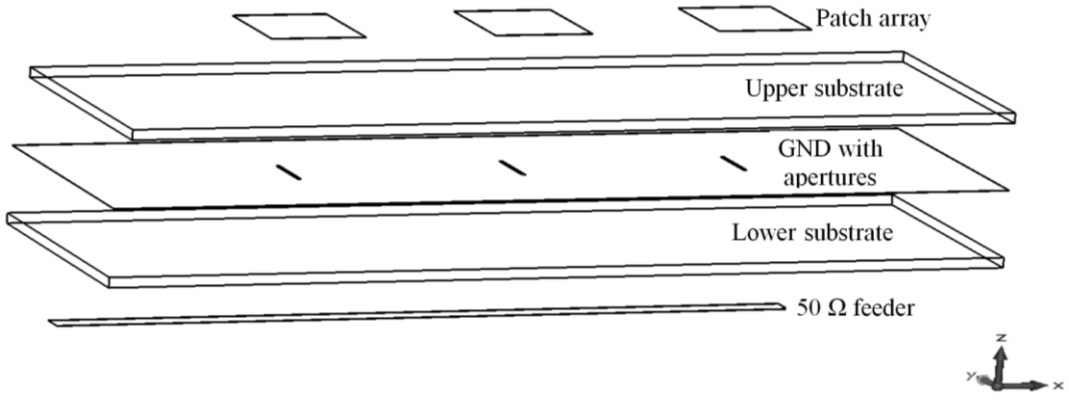

Figure 4.1 Filtering antenna array fed by apertures

The array is fabricated from two dielectric substrates covered by a metallic foil on both the surfaces. The central metallic layer is shared by both the substrates. On the bottom of the substrate, the 50 Ω metallic feeder is created (see Figure 4.1). On the centre metallic layer, apertures are etched into the ground plane. On the top layer, metallic rectangular patches play the role of radiators (see Figure 4.1).

4.2 Patch antenna fed by aperture

In the first step, we designed a single patch at the frequency 5.80 GHz [26]–[30]

$$W_a = \frac{c}{2 \cdot f_0 \cdot \sqrt{\varepsilon_r}}, \tag{1}$$

$$L_a = 0.957 \cdot W_a. \tag{2}$$

An antenna was designed for the substrate ARLON 25N with relative permittivity ε_r = 3.38, thickness h = 1.524 mm and negligible losses. In equations, W_a is the width and L_a is the length of a patch antenna, c is the speed of the light in free space, f_0 is resonant frequency and ε_r is relative permittivity.

In the next step, we add an aperture and a feeder under the antenna. The width of the feeder is 3.30 mm and the length of the open end is the quarter of the wavelength.

4.3 Parameters versus dimensions of antenna

For an easier design of the filtering array fed by apertures, we have to understand the influence of dimensions of the antenna structure on a resonant frequency, a frequency bandwidth, a coupling between the feeder and the patch and a mutual capacitance between the feeder and the patch. In the following parts, we will vary the length and the width of the aperture (slot) and the length of the open end of the feeder. The initial dimensions of the whole structure are W_a = 13.28 mm, L_a = 12.70 mm, W_s = 1.00 mm, L_s = 7.60 mm, w = 3.30 mm, and l_o = 8.80 mm. These dimensions of the patch antenna fed by aperture correspond to the critical coupling (the best matching).

The width of the aperture (slot) was varied form 0.60 mm to 2.60 mm with the step 0.20 mm. The width of the slot W_s has no a dramatic effect on the shift of the resonant frequency, but influences the coupling between the patch and the feeder.

In order to use the equivalent circuit for the synthesis of the filtering antenna, we have to know the specific value of the mutual capacitance and the value of the inverter simulating the coupling. The effect of the width of the slot W_s on the mutual capacitance can be described by

$$C_m = -1.640 \cdot 10^2 \cdot W_N^2 + 1.070 \cdot 10^1 \cdot W_N + 2.026, \tag{3}$$

and the influence on the value of the inverter by

$$J = 7.894 \cdot 10^{-1} \cdot W_N - 1.115 \cdot 10^{-2}. \tag{4}$$

With respect to easier future implementation, the width of the aperture W_s is normalized by width of the patch antenna $W_N = W_s / W_a$ in equations (3) and (4).

The length of the slot L_s was varied from 6.60 mm to 9.00 mm with the step 0.20 mm. The variation of the parameter L_s has a similar effect as the parameter W_s.

The length of the open end l_o of the feeder under the patch antenna was varied from 6.50 mm to 11.50 mm with the step 0.50 mm. The resonant frequency does not depend on the length of the open end l_o. The parameter l_o influences the coupling between the patch antenna and the feeder.

4.4 Antenna array fed by apertures

In order to verify the properties of the structure of interest, we designed a synchronously tuned three-element antenna array fed by apertures (all the patches are tuned at the same frequency and all the apertures have the same dimensions as well), which is shown in Figure 4.1. The array did not exhibit parasitic resonances and the main lobe direction stayed perpendicular to the substrate within the operation band (see Figure 4.2).

A distance between neighboring patches is one wavelength, approximately. In phase feeding of patches ensures the main lobe direction being perpendicular to the substrate. The length of patches is L_a = 12.7 mm, and the width of patches equals to W_a = 13.3 mm. Slots are L_s = 6.4 mm long and W_s = 0.6 mm wide. The microstrip feeder is designed to exhibit the characteristic impedance Z_0 = 50 Ω (w = 3.3 mm). The length of the open end l_o equals to the quarter of the wavelength, approximately.

The designed antenna array fed by apertures was analyzed by CST Microwave Studio. Figure 4.2 (left) shows that the array is designed for the frequency 5.58 GHz. The 10 dB frequency bandwidth of the array is about 3 % and reflection coefficient is better than –42 dB. No parasitic resonances appear in the operation band.

The frequency response of a normalized realized gain creates an equivalent of a band-pass filter (left part in Figure 4.2). For the gain, the 3 dB frequency bandwidth is 8 % wide, and the maximal realized gain is 10.8 dBi.

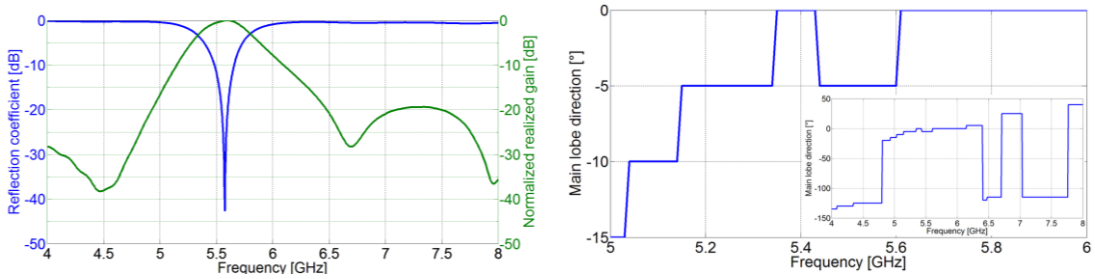

Figure 4.2 Frequency responses of S_{11} and normalized realized gain in direction perpendicular to substrate (left) and main lobe direction (right) of synchronously tuned three-element filtering patch array fed by apertures

Selectivity of the equivalent band-pass filter is better than 36.6 dB/GHz. Suppression in the stop band equals to 20 dB. Figure 4.2 (left) shows that the three-element filtering array fed by apertures radiates in the frequency range from 5.15 GHz to 6.14 GHz only. The main lobe direction varies from –5° to 0° (right part in Figure 4.2).

As demonstrated in this Section, the antenna array fed by apertures is a good candidate for design of the filtering array since this structure meets our demands on the number of resonances, frequency selectivity and direction of the main lobe very well.

5 EQUIVALENT CIRCUIT OF FILTERING ANTENNA ARRAY FED BY APERTURES

In this Section, we will introduce an equivalent circuit of the single patch antenna fed by aperture which will be compared with the results of the full-wave simulation of the same structure. The equivalent circuit of the three-element filtering patch antenna array fed by apertures will be introduced as well and we will derive formulas for obtaining the requested frequency response of the reflection coefficient. Derived formulas will be implemented in MATLAB. The results calculated in MATLAB, simulated as the equivalent circuit and the full-wave model will be mutually compared. A transformation of an equivalent-circuit model of the filtering patch array fed by apertures to a normalized low-pass prototype filter will be introduced.

5.1 Equivalent circuit of single patch antenna fed by aperture

An equivalent circuit of the patch fed by aperture is depicted in Figure 5.1 (left). Values of a parallel resonant circuit *RLC* represent the patch antenna only. The capacitance C_m is a mutual capacitance between the feeder and the patch, and *JINV* denotes an admittance inverter (*J*-inverter) between the feeder and the patch.

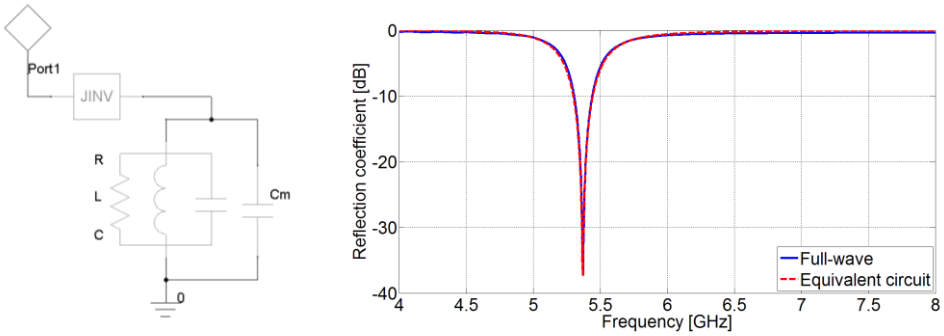

Figure 5.1 The equivalent circuit of the patch fed by aperture:
ANSYS Designer model (left) and comparison of the reflection coefficient of the full-wave model versus equivalent circuit (right)

The comparison of the S_{11} of the full-wave model of the patch antenna fed by aperture from CST with the equivalent circuit is depicted in Figure 5.1 (right). The results are in a good agreement, and therefore, the equivalent circuit can be used as a complete equivalent model of the filtering array for future filter design approach.

5.2 Equivalent circuit of filtering patch array fed by apertures

An equivalent model of the filtering antenna will be derived for the three-element filtering patch array fed by apertures which is shown in Figure 5.2 (left). This equivalent circuit can be extended to higher orders by following the same principle. The equivalent circuit is composed of three parallel *RLC* resonant circuits, three mutual capacitances

C_m, three *J*-inverters and four segments of a transmission line. The parallel *RLC* resonant circuits simulate the behavior of the patches. In order to meet outputs of full-wave simulations, parameters of the *RLC* resonator were set to R = 50.4 Ω, L = 66.2 pH, C = 11.4 pF and C_m = 1.8 pF.

The *J*-inverter simulates coupling between the microstrip transmission line (feeder) and the individual patch. The coupling equals to 0.0162. The width of the microstrip feeder is 3.3 mm, and its characteristic impedance equals to 50 Ω. The lengths of the first, the second and the third segment of the feeder are 30 mm. The length of the last segment of the feeder (from the last patch to the open end) is 8.8 mm.

The equivalent circuit was verified in a circuit simulator of ANSYS Designer and in MATLAB by a script exploiting *ABCD* matrices [31] – [35]. The *ABCD* matrix of the transmission line follows [31]

$$\begin{bmatrix} A & B \\ C & D \end{bmatrix} = \begin{bmatrix} \cos(\beta \cdot l) & j \cdot Z_c \cdot \sin(\beta \cdot l) \\ j \cdot Y_c \cdot \sin(\beta \cdot l) & \cos(\beta \cdot l) \end{bmatrix}. \tag{5}$$

The *ABCD* matrix for a parallel combination of resonant circuits and *J*-inverter can be obtained by [31]

$$\begin{bmatrix} A & B \\ C & D \end{bmatrix} = \begin{bmatrix} 1 & 0 \\ \dfrac{j \cdot \omega \cdot R \cdot L \cdot J^2}{R - \omega^2 \cdot R \cdot L \cdot C + j \cdot \omega \cdot L} & 1 \end{bmatrix}. \tag{6}$$

In the next step, we can calculate the total *ABCD* matrix of the equivalent circuit of the whole antenna structure by multiplying equations (5) and (6).

The reflection coefficient of the equivalent circuit may be calculated from the total *ABCD* matrix by using [31], [32]

$$S_{11} = \frac{A + B \cdot Y_0 - C \cdot Z_0 - D}{A + B \cdot Y_0 + C \cdot Z_0 + D}. \tag{7}$$

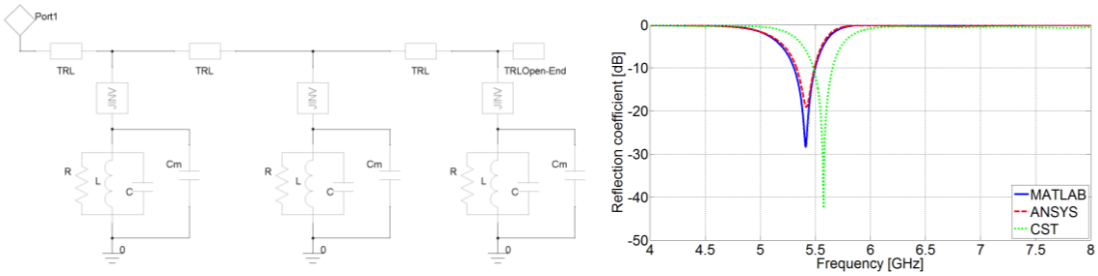

Figure 5.2 Equivalent circuit of three-element filtering patch array fed by apertures: ANSYS Designer model (left) and comparison of the full-wave model implemented in CST Microwave Studio, the equivalent-circuit model implemented in ANSYS Designer, and the equivalent-circuit model implemented in MATLAB (right)

Figure 5.2 (right) compares results of full-wave analysis in CST Microwave Studio (green line), results of circuit analysis in ANSYS Designer (red line) and results of MATLAB computations (blue line). Obviously, frequency responses of reflection coefficient computed in ANSYS Designer and MATLAB script agree well.

The frequency shift between the full-wave model and the equivalent circuit from MATLAB is 2.5 %, approximately. Matching of the full-wave model is better about 15 dB compared with the equivalent-circuit model implemented in MATLAB.

Hence, the equivalent circuit model is proven to fully replace the full-wave model in faster, less accurate calculations.

5.3 Low-pass transformation

In this Chapter, we present a transformation of an equivalent-circuit model of the patch array fed by apertures to a normalized low-pass prototype filter. The transformation is given by the relation [31] and [32]

$$g = C \cdot \frac{FBW \cdot \omega_0}{\Omega_C} . \tag{8}$$

Using the above-described process and considering (8), we can move the capacitances *g* before the *J*-inverters. Thanks to this change, the capacitances *g* will be transformed to the inductances *gg* (left part in Figure 5.3). Now, the frequency response of the reflection coefficient of the one-port configuration of the low-pass prototype filter can be calculated by a script in MATLAB (right part in Figure 5.3). The environment plays the role of the second port as in the previous case.

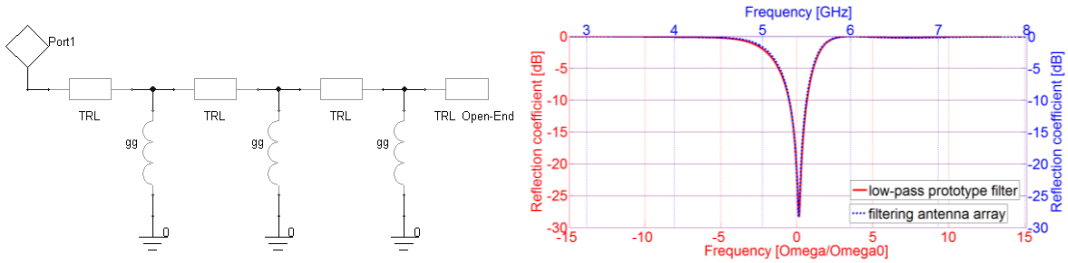

Figure 5.3 Equivalent circuit of the low-pass prototype filter (left) and comparison of the frequency response of the S_{11} of the equivalent circuit of the three-element filtering array with the response of the low-pass prototype filter (right)

Figure 5.3 (right) shows the frequency response of the S_{11} of the equivalent circuit of the three-element filtering array (left part in Figure 5.2) which was calculated by the script in MATLAB using equations and principles described above. This response is depicted by the doted blue line and corresponding scales are shown in blue.

The frequency response of the S_{11} of the recalculated low-pass prototype filter (solid red line) which was calculated by script in MATLAB and which corresponds with Figure 5.3 (left) is illustrated in Figure 5.3 (right) as well. The response is located to bottom and left axes.

Figure 5.3 (right) shows that the frequency response of the S_{11} of the equivalent circuit is identical with the response of the low-pass prototype filter. Therefore, the proposed process can be used for the complete design of the filtering antenna array.

6 SYNTHESIS OF FILTERING ANTENNA ARRAY FED BY APERTURES

In this Section, we introduce a main idea for a comprehensive synthesis of the filtering antenna array. The synthesis procedure combines the frequency filter design and the antenna design approaches. The frequency response of the reflection coefficient at the antenna input, the frequency response of the normalized realized gain, and the direction of the main lobe are objectives of this synthesis. The desired center frequency, the requested fractional bandwidth of the filtenna and the prescribed magnitude of the reflection coefficient at the input of the filtenna have to be given to evaluate objectives.

6.1 Main idea of synthesis of filtering antenna array fed by apertures

The main idea of synthesis of the filtering array is based on the equation [26]

$$|S_{21RG}| = D \cdot AF \cdot \left(1 - |S_{11}|^2\right). \tag{9}$$

Here, S_{21RG} is the frequency response of the normalized realized gain, which is understood as an equivalent of the frequency response of the transmission coefficient of the frequency filter (the second port of the filter is replaced by the radiation of the antenna to the surrounding environment).

Equation (9) shows that the parameter S_{21RG} depends on the directivity of the single antenna D [25]–[28], on the array factor AF of the whole structure [36]–[38] and on the frequency response of the reflection coefficient at the antenna input S_{11} [31], [39].

The formula (9) can be rewritten to the equation [26]

$$|S_{21RG}| = D \cdot AF \cdot \left|S_{21}'\right|^2 \cdot \tag{10}$$

Here, S_{21}' corresponds to losses in dielectrics and losses by the radiation [25] and [26].

When synthesizing a filter, g_i coefficients of the low-pass prototype filter can shape the frequency response of the reflection coefficient S_{11} and the transmission coefficient S_{21}'. Obviously, we can shape the frequency response of the normalized realized gain S_{21RG} a similar way.

Since conventional approximations of filter characteristics (Chebyshev, Butterworth, etc.) are not applicable in case of filtering arrays, alternative coefficients will be derived in the next Section.

6.2 Filter approach for obtain values of the equivalent circuit

In this Section, we discuss the filter approach and equations which are necessary to design of the filtering antenna array and for control of the shapes of the frequency response of the reflection coefficient.

For computing the filtering antenna array, where each individual patch antenna, (combination of *RLC* in the equivalent circuit) are tuned at different frequencies $f_{0a}(i)$, we use theory implemented on asynchronously tuned filters [31]

$$f_{0a}(i) = f_0 \pm \frac{FBW \cdot f_0}{2}, \tag{11}$$

where $f_{0a}(i)$ is individual asynchronously tuned resonant frequency, *FBW* is the fractional bandwidth between resonant frequencies $f_{0a}(i)$ and f_0 is the center frequency of the whole filtering antenna array.

Capacitances and inductances of parallel resonant circuits modeling patches in the filtering array can be evaluated by [31]

$$C(i) = \frac{1}{2 \cdot \pi \cdot f_{0a}(i) \cdot R \cdot FBW_a}, \tag{12}$$

$$L(i) = \frac{1}{(2 \cdot \pi \cdot f_{0a}(i))^2 \cdot C(i)}. \tag{13}$$

For evaluating *J*-inverters among individual patches and feeder, we can use [31]

$$J(i) = \sqrt{\frac{Y_0 \cdot C(i) \cdot FBW \cdot 2 \cdot \pi \cdot f_0}{\Omega_C \cdot g_0 \cdot g_i}}. \tag{14}$$

From the value of the *J*-inverters (14) and the dependencies of the mutual capacitance and coupling on the width of the aperture W_s, we can calculate mutual capacitances between patch antenna and feeder by using (3) and (4)

$$C_m(i) = -1.640 \cdot 10^2 \cdot \left(\frac{J(i) + 1.115 \cdot 10^{-2}}{7.894 \cdot 10^{-1}} \right)^2 + 1.070 \cdot 10^1 \cdot \frac{J(i) + 1.115 \cdot 10^{-2}}{7.894 \cdot 10^{-1}} + 2.026, \tag{15}$$

where *R* denotes value of the resistor, $C(i)$ and $L(i)$ are individual capacitance and individual inductance and $C_m(i)$ is individual mutual capacitance in the parallel combination of *RLC* in Figure 5.2 (left). The value of the fractional bandwidth of a single patch antenna fed by an aperture is denoted as FBW_a, Y_0 represents the characteristic admittance of the microstrip feeder, g_0 and g_i are coefficients of the low-pass prototype filter and Ω_C is the cutoff angular frequency of the filter.

6.3 Synthesis of frequency response of normalized realized gain

The equivalent model of the filtering array fed by apertures and synthesis of the reflection coefficient were described in the detail in previous Section and in [39], [40]. In this Section, the synthesis of the frequency response of the normalized realized gain based on the equivalent model, the frequency response of the reflection coefficient and calculation of a radiation pattern based on the electric surface current is presented. This approach is calculated by script in MATLAB and compared with the results from CST.

In order to calculate the frequency response of the normalized realized gain of the filtering antenna, we have to consider [28]

$$\begin{aligned} |E_\Theta(\Theta)|^2 = {} & \varepsilon_{eff} \cdot \left[1 + \varepsilon_r \cdot \cot^2\left(k_0 \cdot h \cdot \sqrt{\varepsilon_r}\right)\right] \frac{\cos^2\left(k_0 \cdot L_a \cdot \sin\Theta / 2\right)}{\left(\varepsilon_{eff} - \sin^2\Theta\right)^2} \cdots \\ & \frac{\left(\varepsilon_{eff} - \sin^2\Theta\right) \cdot \cos^2\Theta}{\left(\varepsilon_{eff} - \sin^2\Theta\right) + \varepsilon_r^2 \cdot \cos^2\Theta \cdot \cot^2\left(k_0 \cdot h \cdot \sqrt{\varepsilon_r - \sin^2\Theta}\right)} \end{aligned} \tag{16}$$

to describe the radiation pattern of a patch antenna in the E-plane, and [28]

$$|E_{\Phi}(\Theta)|^2 = \left[1+\varepsilon_r \cdot \cot^2\left(k_0 \cdot h \cdot \sqrt{\varepsilon_r}\right)\right]\sin c^2\left(k_0 \cdot W_a \cdot \sin\cdot \Theta/2\right)... \\ \frac{\cos^2\Theta}{\left(\varepsilon_r - \sin^2\Theta\right)\cot^2\left(k_0 \cdot h \cdot \sqrt{\varepsilon_r - \sin^2\Theta}\right)+\cos^2\Theta} \tag{17}$$

to describe the radiation pattern of a patch antenna in the H-plane.

Here, ε_r denotes a relative permittivity of the substrate, h is a thickness of the substrate, ε_{eff} is an effective dielectric constant, k_0 is the free-space wave number, L_a is the length of the patch and W_a is the width of the patch.

Following [28], directivity can be calculated by equation

$$D = \frac{4 \cdot \pi \cdot r^2\left(|E_{\Theta}|^2 + |E_{\Phi}|^2\right)_{\Theta=0}}{2 \cdot \eta_0 \cdot P_r} \tag{18}$$

using equations (16) and (17). Here, r corresponds to a distance of some point outside the patch antenna, E_{Θ} is the radiation pattern of the patch antenna in the E-plane and E_{Φ} is the radiation pattern of the patch antenna in the H-plane, η_0 is the impedance of the free space ($120\pi\ \Omega$) and P_r is a radiated power.

In order to calculate a total radiation pattern of the filtering array represented by the equivalent circuit (Figure 4.1 and left part in Figure 5.2) [39], an array factor has to be defined [25], [26]

$$AF = \frac{\sin\left(N \cdot \Psi/2\right)}{\sin\left(\Psi/2\right)}, \tag{19}$$

where N is a number of the radiation elements and the definition of Ψ is following [25]

$$\Psi = k_0 \cdot d \cdot \cos\Theta + \xi\,. \tag{20}$$

In equation (20), k_0 is the free-space wave number, d is a distance between two neighboring radiation elements and ξ is a phase shift between two adjacent patches.

In order to obtain the frequency response of the normalized realized gain, the frequency response of the reflection coefficient [31], [39] has to be included.

Figure 6.1 shows a comparison of the frequency response of the normalized realized gain obtained by the full-wave model in CST Microwave Studio with the result achieved by script in MATLAB which was described above. Obviously, the center frequency of the equivalent circuit is shifted down about 280 MHz. The dynamics of the filtering antenna array is approximately same in both the cases as well as the 3 dB fractional frequency bandwidth.

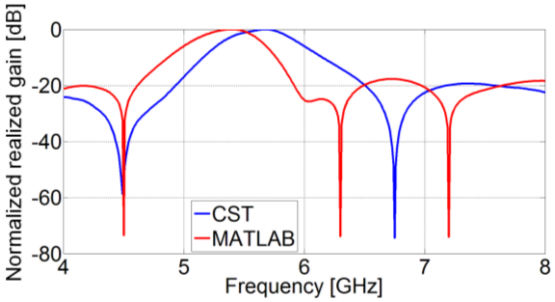

Figure 6.1 Comparison of the frequency response of the normalized realized gain obtained by CST Microwave Studio (blue) and by MATLAB (red)

6.4 New g_i coefficients for filtering antenna arrays

This Section is focused on the definition of new g_i coefficients of three-element and four-element filtering antenna arrays fed by apertures. New g_i coefficients enable us to control frequency responses of the reflection coefficient and the normalized realized gain. The coefficients are extracted for a specific value of the reflection coefficient and an acceptable value of the fractional bandwidth of the filtering array. The g_i coefficients are obtained by the optimization of the shape of the frequency responses of the reflection coefficient and the normalized realized gain by using a script in MATLAB which includes the equations described in the previous Sections.

6.4.1 Three-element filtering antenna array and g_i coefficients

The new g_i coefficients for the three-element filtering antenna array fed by apertures, which are defined for several input parameters, are published in this Subsection. The equation

$$FBW = \frac{-5.598\cdot10^{-1}+\sqrt{\left(5.598\cdot10^{-1}\right)^2-4\cdot6.303\cdot\left(6.809\cdot10^{-2}-FBW_s\right)}}{2\cdot6.303} \tag{21}$$

describes the relationship between the fractional bandwidth of the whole structure FBW_s and the fractional bandwidth between the resonant frequencies $f_{0d}(i)$ of the individual patches (FBW). The equation (21) is derived for the acceptable reflection coefficient (in this case $S_{11} < -10$ dB).

In (21), FBW_s represents the fractional bandwidth of the whole structure, which is related to the frequency response of the normalized realized gain (transmission coefficient in the filter theory) for the decrease by 3 dB. In this case, the fractional bandwidth FBW_s can be set in the interval from 7 % up to 14 %.

Equations

$$g_0 = g_4 = 1, \tag{22}$$

$$g_1 = g_3 = -4.778\cdot10^2\cdot FBW^2 + 5.506\cdot10^1\cdot FBW - 5.333\cdot10^{-2}, \tag{23}$$

$$g_2 = -5.097\cdot10^2\cdot FBW^2 + 5.536\cdot10^1\cdot FBW + 1.533\cdot10^{-1} \tag{24}$$

provide us the definition of the g_i coefficients of the three-element filtering antenna array. Equation (22) has the same validity for all cases of the acceptable levels of the reflection coefficient.

In equations (22) to (24), the value of the coefficient g_0 is related to a normalized impedance of the transmission line, and the value of the coefficient g_4 corresponds to the impedance of the open end of the transmission line. Thanks to coefficients g_1 and g_3, we can influence the final value of the first and the third J-inverter (the shape of the required parameters such as S_{11} and S_{21RG}). Thanks to the coefficient g_2, final value of the second J-inverter can be reached (the shape of S_{11} and S_{21RG}).

The formulas (21), (23) and (24) have to be recalculated if the required match should be better than $S_{11} < -15$ dB

$$FBW = \frac{-5.495\cdot10^{-1}+\sqrt{\left(5.495\cdot10^{-1}\right)^2-4\cdot6.261\cdot\left(7.445\cdot10^{-2}-FBW_s\right)}}{2\cdot6.261}, \tag{25}$$

$$g_1 = g_3 = -3.727\cdot10^2\cdot FBW^2 + 4.402\cdot10^1\cdot FBW - 5.733\cdot10^{-2}, \tag{26}$$

$$g_2 = -3.329 \cdot 10^2 \cdot FBW^2 + 4.149 \cdot 10^1 \cdot FBW + 2.510 \cdot 10^{-1}, \quad (27)$$

or better than $S_{11} < -20$ dB

$$FBW = \frac{-5.209 \cdot 10^{-1} + \sqrt{\left(5.209 \cdot 10^{-1}\right)^2 - 4 \cdot 6.344 \cdot \left(7.942 \cdot 10^{-2} - FBW_s\right)}}{2 \cdot 6.344}, \quad (28)$$

$$g_1 = g_3 = -2.835 \cdot 10^2 \cdot FBW^2 + 3.592 \cdot 10^1 \cdot FBW - 5.333 \cdot 10^{-3}, \quad (29)$$

$$g_2 = -4.484 \cdot 10^2 \cdot FBW^2 + 5.044 \cdot 10^1 \cdot FBW - 1.117 \cdot 10^{-2}. \quad (30)$$

6.4.2 Four-element filtering antenna array and g_i coefficients

New g_i coefficients for the four-element filtering antenna array fed by apertures are presented is this Section. As in the case of the three-element filtering antenna array, the g_i coefficients are defined for several cases of the input parameters. Concretely, the fractional bandwidth and level of the reflection coefficient are changed.

The equation

$$FBW = \frac{-1.981 + \sqrt{1.981^2 - 4 \cdot \left(-1.770 \cdot 10^1\right) \cdot \left(6.892 \cdot 10^{-2} - FBW_s\right)}}{2 \cdot \left(-1.770 \cdot 10^1\right)} \quad (31)$$

describes the relationship between the fractional bandwidth of the whole structure FBW_s and the fractional bandwidth between the resonant frequencies $f_{0a}(i)$ of individual patches (FBW) for case of the four-element filtenna and $S_{11} < -10$ dB.

In equation

$$g_0 = g_5 = 1, \quad (32)$$

the values of coefficients g_0 and g_5 correspond to a normalized impedance of the feeder (transmission line) and the impedance of the open end of the transmission line. The equation (32) is shared for all cases of the acceptable level of the reflection coefficient which are presented in the next part of this Section.

Thanks to the coefficients g_1 and g_4

$$g_1 = g_4 = 1.354 \cdot 10^2 \cdot FBW^2 + 1.173 \cdot 10^1 \cdot FBW + 3.143 \cdot 10^{-1}, \quad (33)$$

we can influence the final value of the first and the fourth J-inverter (the shape of the required parameters S_{11} and S_{21RG}).

Thanks to the coefficients g_2 and g_3

$$g_2 = g_3 = 3.257 \cdot 10^2 \cdot FBW^2 + 1.759 \cdot FBW + 3.708 \cdot 10^{-1}, \quad (34)$$

the final value of the second and third J-inverter can be reached, and the shape of S_{11} and S_{21RG} can be formed.

The equations (31), (33) and (34) describe the dependence of the fractional bandwidth of the whole structure FBW_s, the coefficients g_1 and g_4, and the coefficients g_2 and g_3 on the fractional bandwidth FBW between two resonant frequencies $f_{0a}(i)$.

Equations (31), (33) and (34) have to be recalculated if the requested matching should be better than $S_{11} < -15$ dB

$$FBW = \frac{-1.429 + \sqrt{1.429^2 - 4 \cdot \left(-1.105 \cdot 10^1\right) \cdot \left(7.171 \cdot 10^{-2} - FBW_s\right)}}{2 \cdot \left(-1.105 \cdot 10^1\right)}, \quad (35)$$

$$g_1 = g_4 = -1.779 \cdot 10^2 \cdot FBW^2 + 3.600 \cdot 10^1 \cdot FBW + 7.762 \cdot 10^{-2}, \quad (36)$$

$$g_2 = g_3 = 1.647 \cdot 10^2 \cdot FBW^2 + 1.643 \cdot 10^1 \cdot FBW + 2.331 \cdot 10^{-1}, \tag{37}$$

or better than $S_{11} < -20$ dB

$$FBW = \frac{-8.417 \cdot 10^{-1} + \sqrt{\left(8.417 \cdot 10^{-1}\right)^2 - 4 \cdot \left(-2.931\right) \cdot \left(7.608 \cdot 10^{-2} - FBW_s\right)}}{2 \cdot \left(-2.931\right)}, \tag{38}$$

$$g_1 = g_4 = -3.038 \cdot 10^2 \cdot FBW^2 + 4.872 \cdot 10^1 \cdot FBW - 3.905 \cdot 10^{-2}, \tag{39}$$

$$g_2 = g_3 = 6.075 \cdot 10^1 \cdot FBW^2 + 2.701 \cdot 10^1 \cdot FBW + 1.471 \cdot 10^{-1}. \tag{40}$$

6.5 Dimensions of the full-wave model

The following paragraphs are focused on the way to obtain the final dimensions of the filtering antenna array fed by apertures. The length and the width of the each individual patch antenna can be calculated by equations (1) and (2), which were presented in Section 4.2. The width of the each aperture (slot) can be calculated by

$$W_s(i) = \frac{c \cdot \left(J(i) + 1.115 \cdot 10^{-2}\right)}{7.894 \cdot 10^{-1} \cdot 2 \cdot f_{0a}(i) \cdot \sqrt{\varepsilon_r}} \tag{41}$$

and the length of the aperture by

$$L_s(i) = \frac{0.572 \cdot c}{2 \cdot f_{0a}(i) \cdot \sqrt{\varepsilon_r}}. \tag{42}$$

Other parameters (the width of the feeder, the distance between two neighboring patch antennas and the length of the open end of the feeder) can be calculated to using fundamental equations from [31], [32].

6.6 Comparison of theoretical results and full-wave results

In this Section, the complete synthesis of the filtering antenna array fed by apertures is confronted with the full-wave results obtained by CST Microwave Studio. These comparisons are done for the three-element filtenna and for the four-element filtering array. In comparisons, several cases of input settings with different values of the center frequency f_0, the fractional bandwidth of the whole structure FBW_s and the acceptable level of the reflection coefficient S_{11} are assumed. Compared models do not consider a connector, losses in the dielectrics and adhesives between substrates.

6.6.1 Full-wave verification of the three-element filtering antenna array

The described process of the design methodology of the three-element filtering antenna array is verified on three different test cases over the frequency band from 4.8 GHz to 6.8 GHz; for the fractional bandwidth from 7 % to 14 % and for the level of the reflection coefficient from –10 dB to –20 dB.

The first verification of the design methodology was carried out for: f_0 = 4.8 GHz; FBW_s = 10 % and S_{11} < –10 dB. Table 6.1 summarizes component values of the equivalent circuit model (left), dimensions of planar implementation (center) and optimized implementation (right).

Table 6.1 Values of elements in equivalent circuit of filtenna (left), dimensions of planar implementation of filtenna (center), dimensions of optimized filtenna (right); three-element filtenna; f_0 = 4.8 GHz; FBW_s = 10 % and S_{11} < –10 dB

Equivalent circuit				Dimensions from script [mm]				CST optimized [mm]			
L_1, L_3 [pH]	74.45	L_2 [pH]	77.44	W_{a1}, W_{a3}	15.15	W_{a2}	15.76	W_{a1}, W_{a3}	15.15	W_{a2}	15.76
C_1, C_3 [pF]	11.74	C_2 [pF]	12.21	L_{a1}, L_{a3}	14.50	L_{a2}	15.09	L_{a1}, L_{a3}	14.50	L_{a2}	15.09
J_1, J_3 [mS]	14.90	J_2 [mS]	14.40	W_{s1}, W_{s3}	0.50	W_{s2}	0.51	W_{s1}, W_{s3}	0.50	W_{s2}	0.51
C_{m1}–C_{m3} [pF]	2.20	d [mm]	32.20	L_{s1}, L_{s3}	8.67	L_{s2}	9.02	L_{s1}, L_{s3}	8.35	L_{s2}	8.67
R_1–R_3 [Ω]	50.37	l_o [mm]	9.50	d	32.20	l_o	9.50	d	34.70	l_o	9.51

In Figure 6.2 (left), frequency responses of S_{11} at the filtenna input and transmission coefficient (normalized realized gain RG) are depicted. Comparison of the main lobe direction calculated by script in MATLAB with the result obtained by CST Microwave Studio is shown in Figure 6.2 (right). Results are in a good agreement.

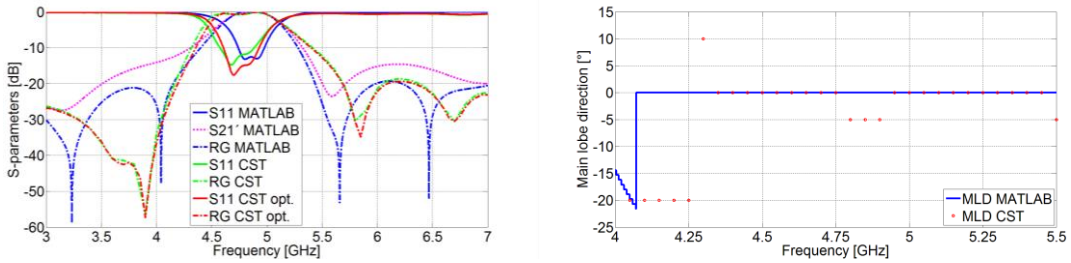

Figure 6.2 Frequency responses of reflection coefficient S_{11}, transmission coefficient S_{21} for equivalent circuit, planar implementation and optimized planar implementation (left) and frequency responses of the main lobe direction (right) for the case: three-element filtenna; f_0 = 4.8 GHz; FBW_s = 10 % and S_{11} < –10 dB

In the second test case, the filtenna was designed for: f_0 = 5.8 GHz; FBW_s = 13 % and S_{11} < –15 dB. Table 6.2 summarizes values of the equivalent circuit model (left), dimensions of planar implementation (center) and optimized implementation (right).

Table 6.2 Values of elements in equivalent circuit of filtenna (left), dimensions of planar implementation of filtenna (center), dimensions of optimized filtenna (right); three-element filtenna; f_0 = 5.8 GHz; FBW_s = 13 % and S_{11} < –15 dB

Equivalent circuit				Dimensions from script [mm]				CST optimized [mm]			
L_1, L_3 [pH]	61.00	L_2 [pH]	64.77	W_{a1}, W_{a3}	12.42	W_{a2}	13.18	W_{a1}, W_{a3}	12.21	W_{a2}	12.96
C_1, C_3 [pF]	9.62	C_2 [pF]	10.21	L_{a1}, L_{a3}	11.88	L_{a2}	12.62	L_{a1}, L_{a3}	11.68	L_{a2}	12.40
J_1, J_3 [mS]	19.30	J_2 [mS]	17.90	W_{s1}, W_{s3}	0.48	W_{s2}	0.48	W_{s1}, W_{s3}	0.47	W_{s2}	0.46
C_{m1}–C_{m3} [pF]	2.19	d [mm]	27.10	L_{s1}, L_{s3}	7.11	L_{s2}	7.55	L_{s1}, L_{s3}	7.12	L_{s2}	7.32
R_1–R_3 [Ω]	50.37	l_o [mm]	8.00	d	27.10	l_o	8.00	d	28.60	l_o	7.43

In Figure 6.3 (left), frequency responses of reflections and transmissions coefficients of the equivalent circuit model (obtained by script in MATLAB), planar implementation (CST) and optimized implementation (CST opt.) show a good agreement. The maximal deviations of the main lobe are shown in Figure 6.3 (right).

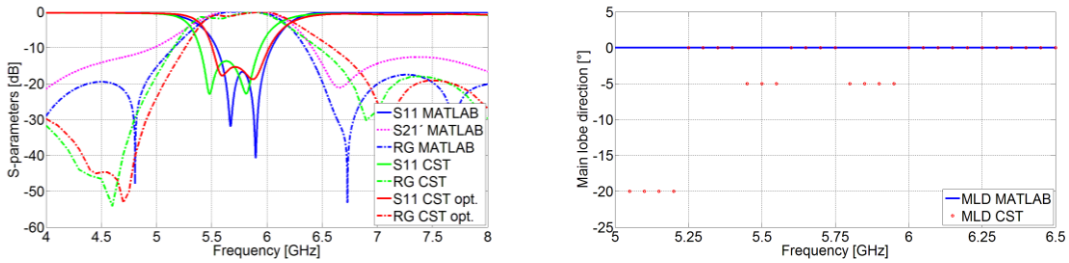

Figure 6.3 Frequency responses of reflection coefficient S_{11}, transmission coefficient S_{21} for equivalent circuit , planar implementation and optimized planar implementation (left) and frequency responses of the main lobe direction (right) for the case: three-element filtenna; f_0 = 5.8 GHz; FBW_s = 13 % and S_{11} < –15 dB

In the third test case, the filtering array was designed for: f_0 = 6.8 GHz; FBW_s = 10 % and S_{11} < –10 dB. Table 6.3 summarizes values of the equivalent circuit model (left), dimensions of planar implementation (center) and optimized implementation (right).

Table 6.3 Values of elements in equivalent circuit of filtenna (left), dimensions of planar implementation of filtenna (center), dimensions of optimized filtenna (right); three-element filtenna; f_0 = 6.8 GHz; FBW_s = 10 % and S_{11} < –10 dB

Equivalent circuit				**Dimensions from script [mm]**				**CST optimized [mm]**			
L_1, L_3 **[pH]**	52.55	L_2 **[pH]**	54.67	W_{a1}, W_{a3}	10.70	W_{a2}	11.13	W_{a1}, W_{a3}	10.54	W_{a2}	10.97
C_1, C_3 **[pF]**	8.29	C_2 **[pF]**	8.62	L_{a1}, L_{a3}	10.24	L_{a2}	10.65	L_{a1}, L_{a3}	10.09	L_{a2}	10.50
J_1, J_3 **[mS]**	14.90	J_2 **[mS]**	14.40	W_{s1}, W_{s3}	0.35	W_{s2}	0.36	W_{s1}, W_{s3}	0.34	W_{s2}	0.37
C_{m1}–C_{m3} **[pF]**	2.20	d **[mm]**	23.40	L_{s1}, L_{s3}	6.12	L_{s2}	6.37	L_{s1}, L_{s3}	6.29	L_{s2}	6.24
R_1–R_3 **[Ω]**	50.37	l_o **[mm]**	6.90	d	23.40	l_o	6.90	d	25.50	l_o	6.67

In Figure 6.4 (left), frequency responses of reflections and transmissions coefficients of the equivalent circuit model (MATLAB), planar implementation (CST) and optimized implementation (CST opt.) show a good agreement. Figure 6.4 (right) compares the frequency responses of the main lobe direction.

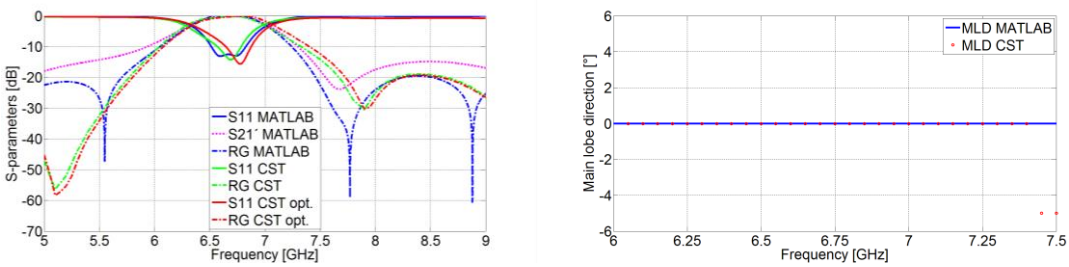

Figure 6.4 Frequency responses of reflection coefficient S_{11}, transmission coefficient S_{21} for equivalent circuit, planar implementation and optimized planar implementation (left) and frequency responses of the main lobe direction (right) for the case: three-element filtenna; f_0 = 6.8 GHz; FBW_s = 10 % and S_{11} < –10 dB

6.6.2 Full-wave verification of the four-element filtering antenna array

The described process of the design methodology of the four-element filtering antenna array is verified on the three different test cases over the frequency band from

4.8 GHz to 6.8 GHz; the fractional bandwidth of the whole structure from 8 % to 12 % and the level of the reflection coefficient from –10 dB to –20 dB.

The first verification of the design methodology was carried out for: f_0 = 4.8 GHz; FBW_s = 8 % and S_{11} < –15 dB. Table 6.4 summarizes values of the equivalent circuit (left), dimensions of planar implementation (center) and optimized one (right).

Table 6.4 Values of elements in equivalent circuit of filtenna (left), dimensions of planar implementation of filtenna (center), dimensions of optimized filtenna (right); four-element filtenna; f_0 = 4.8 GHz; FBW_s = 8 % and S_{11} < –15 dB

Equivalent circuit				Dimensions from script [mm]				CST optimized [mm]			
L_1, L_4 [pH]	75.68	L_2, L_3 [pH]	76.15	W_{a1}, W_{a4}	15.41	W_{a2}, W_{a3}	15.50	W_{a1}, W_{a4}	15.59	W_{a2}, W_{a3}	15.99
C_1, C_4 [pF]	11.93	C_2, C_3 [pF]	12.01	L_{a1}, L_{a4}	14.74	L_{a2}, L_{a3}	14.83	L_{a1}, L_{a4}	14.92	L_{a2}, L_{a3}	15.30
J_1, J_4 [mS]	12.89	J_2, J_3 [mS]	11.96	W_{s1}, W_{s4}	0.47	W_{s2}, W_{s3}	0.45	W_{s1}, W_{s4}	0.43	W_{s2}, W_{s3}	0.43
C_{m1}–C_{m4} [pF]	2.20	d [mm]	34.08	L_{s1}, L_{s4}	8.82	L_{s2}, L_{s3}	8.87	L_{s1}, L_{s4}	8.05	L_{s2}, L_{s3}	8.76
R_1–R_4 [Ω]	50.37	l_o [mm]	9.47	d	34.08	l_o	9.47	d	38.20	l_o	9.51

In Figure 6.5 (left), frequency responses of S_{11} at the filtenna input and transmission coefficient (normalized realized gain RG) are depicted. MATLAB stands for the equivalent circuit approach, CST represents full-wave simulation of the equivalent planar implementation, and CST opt. is the optimized planar implementation. Obviously, all frequency responses exhibit a sufficient agreement. Comparison of the main lobe direction is shown in Figure 6.5 (right).

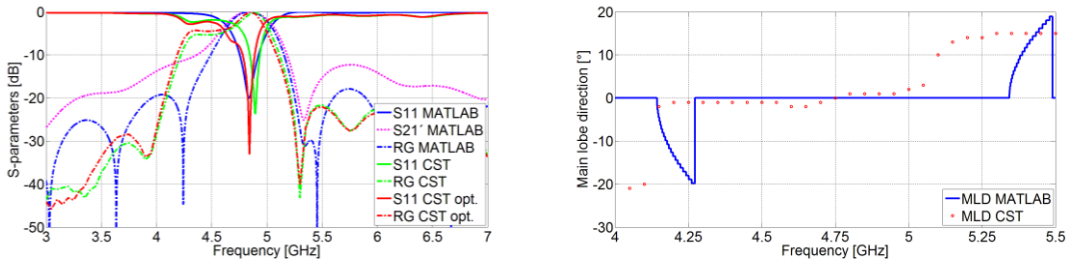

Figure 6.5 Frequency responses of reflection coefficient S_{11}, transmission coefficient S_{21} for equivalent circuit, planar implementation and optimized planar implementation (left) and frequency responses of the main lobe direction (right) for the case: four-element filtenna; f_0 = 4.8 GHz; FBW_s = 8 % and S_{11} < –15 dB

In the second test case, the four-element filtenna was tuned at the center frequency 5.8 GHz with the fractional bandwidth of the whole structure 12 % and the acceptable level of the reflection coefficient better than –10 dB. Table 6.5 summarizes component values of the equivalent circuit model (left), dimensions of planar implementation (center) and optimized implementation (right).

Table 6.5 Values of elements in equivalent circuit of filtenna (left), dimensions of planar implementation of filtenna (center), dimensions of optimized filtenna (right); four-element filtenna; f_0 = 5.8 GHz; FBW_s = 12 % and S_{11} < –10 dB

Equivalent circuit				Dimensions from script [mm]				CST optimized [mm]			
L_1, L_4 [pH]	61.59	L_2, L_3 [pH]	64.12	W_{a1}, W_{a4}	12.54	W_{a2}, W_{a3}	13.05	W_{a1}, W_{a4}	12.61	W_{a2}, W_{a3}	13.16
C_1, C_4 [pF]	9.71	C_2, C_3 [pF]	10.11	L_{a1}, L_{a4}	12.00	L_{a2}, L_{a3}	12.49	L_{a1}, L_{a4}	12.07	L_{a2}, L_{a3}	12.59
J_1, J_4 [mS]	17.65	J_2, J_3 [mS]	18.34	W_{s1}, W_{s4}	0.46	W_{s2}, W_{s3}	0.49	W_{s1}, W_{s4}	0.48	W_{s2}, W_{s3}	0.43
C_{m1}–C_{m4} [pF]	2.20	d [mm]	28.64	L_{s1}, L_{s4}	7.17	L_{s2}, L_{s3}	7.47	L_{s1}, L_{s4}	6.67	L_{s2}, L_{s3}	6.56
R_1–R_4 [Ω]	50.37	l_o [mm]	7.96	d	28.64	l_o	7.96	d	29.40	l_o	8.00

The comparison of the results calculated by script in MATLAB with the results obtained by CST and with optimized results from CST is shown in Figure 6.6 (left). There are the blue lines for results from script in MATLAB, the green lines represent the CST results and the red lines are optimized results from CST. The direction of the main lobe illustrates Figure 6.6 (right). All results are in a good agreement.

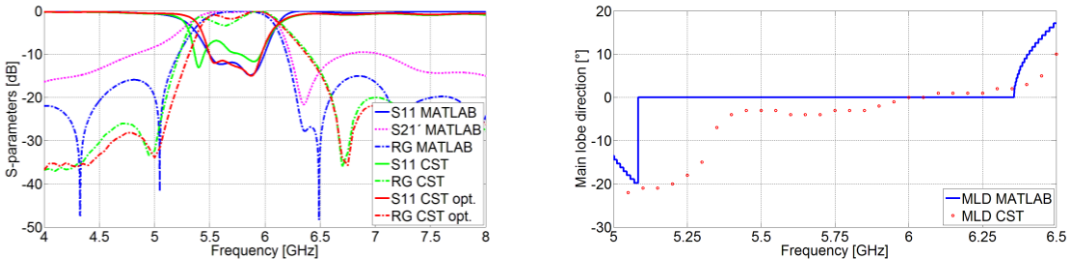

Figure 6.6 Frequency responses of reflection coefficient S_{11}, transmission coefficient S_{21} for equivalent circuit, planar implementation and optimized planar implementation (left) and frequency responses of the main lobe direction (right) for the case: four-element filtenna; f_0 = 5.8 GHz; FBW_s = 12 % and S_{11} < –10 dB

The last test case of the four-element filtering array (f_0 = 6.8 GHz; FBW_s = 12 %; S_{11} < –20 dB) was designed. Table 6.6 summarizes component values of the equivalent circuit (left), dimensions of planar implementation (center) and optimized one (right).

Table 6.6 Values of elements in equivalent circuit of filtenna (left), dimensions of planar implementation of filtenna (center), dimensions of optimized filtenna (right); four-element filtenna; f_0 = 6.8 GHz; FBW_s = 12 % and S_{11} < –20 dB

Equivalent circuit				**Dimensions from script [mm]**				**CST optimized [mm]**			
L_1, L_4 **[pH]**	51.81	L_2, L_3 **[pH]**	55.49	W_{a1}, W_{a4}	10.55	W_{a2}, W_{a3}	11.29	W_{a1}, W_{a4}	10.60	W_{a2}, W_{a3}	11.33
C_1, C_4 **[pF]**	8.17	C_2, C_3 **[pF]**	8.75	L_{a1}, L_{a4}	10.09	L_{a2}, L_{a3}	10.81	L_{a1}, L_{a4}	10.14	L_{a2}, L_{a3}	10.84
J_1, J_4 **[mS]**	16.76	J_2, J_3 **[mS]**	15.71	W_{s1}, W_{s4}	0.37	W_{s2}, W_{s3}	0.38	W_{s1}, W_{s4}	0.37	W_{s2}, W_{s3}	0.36
C_{m1}–C_{m4} **[pF]**	2.20	d **[mm]**	24.82	L_{s1}, L_{s4}	6.04	L_{s2}, L_{s3}	6.46	L_{s1}, L_{s4}	6.05	L_{s2}, L_{s3}	6.10
R_1–R_4 **[Ω]**	50.37	l_o **[mm]**	6.89	d	24.82	l_o	6.89	d	25.40	l_o	6.90

The confrontation of the responses which are calculated by the script in MATLAB with results obtained by CST is shown in Figure 6.7. Obviously, all frequency responses exhibit sufficient agreement.

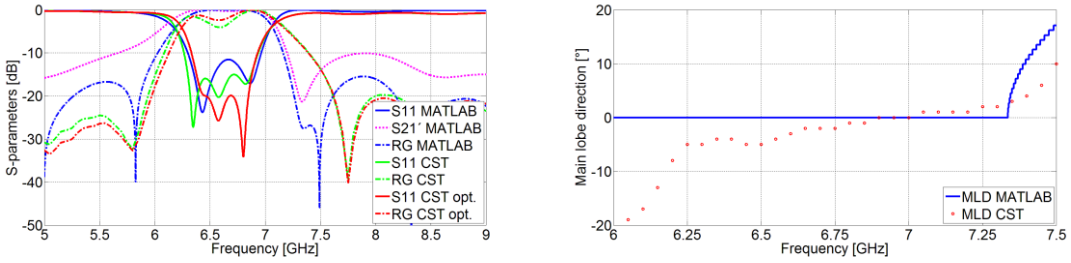

Figure 6.7 Frequency responses of reflection coefficient S_{11}, transmission coefficient S_{21} for equivalent circuit, planar implementation and optimized planar implementation (left) and frequency responses of the main lobe direction (right) for the case: four-element filtenna; f_0 = 6.8 GHz; FBW_s = 12 % and S_{11} < –20 dB

7 VERIFICATION BY MEASUREMENT

This Section is focused on the experimental verification of theoretical results. The verification compares a full-wave model simulated in CST Microwave Studio and experimental results obtained by measurements.

7.1 Verification of the three-element filtering antenna array

Three test cases characterized by different requirements were manufactured and measured. The first sample was designed for: f_0 = 4.8 GHz; FBW_s = 10 %; S_{11} < –10 dB. The comparison of simulated results from CST, where the dielectric losses and the SMA connector were included, with measured results is shown in Figure 7.1 (left).

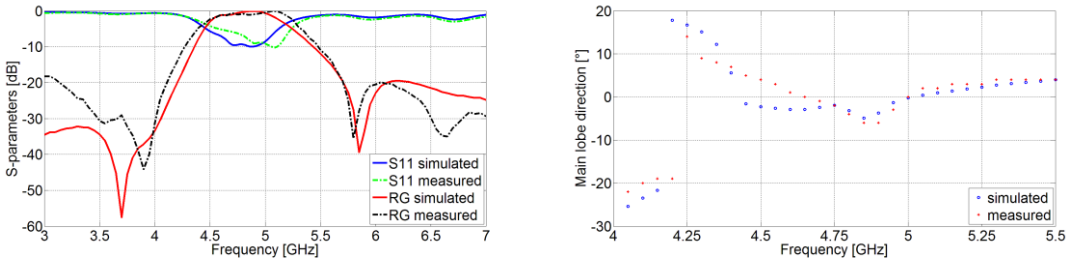

Figure 7.1 Comparison of the simulated and measured frequency responses of reflection coefficient and normalized realized gain (left) and main lobe direction (right) for the case: three-element filtenna; f_0 = 4.8 GHz; FBW_s = 10 %; S_{11} < –10 dB

The frequency response of the main lobe direction is illustrated by Figure 7.1 (right). The simulated and measured co-polarizations and cross-polarizations in the E-plane and the H-plane are shown in Figure 7.2. The realized gain of this filtering antenna array is about 9 dBi over the operating range.

Figure 7.1 and Figure 7.2 shows that simulated results and measured ones are in a good agreement (see Table 7.1).

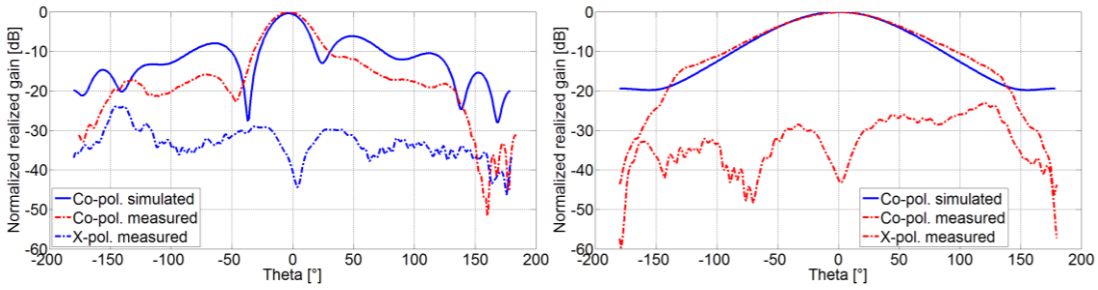

Figure 7.2 Comparison of simulated and measured co and cross polarizations in E-plane (left) and H-plane (right) of the three-element filtenna at frequency 4.8 GHz

Table 7.1 Comparison of the most important simulated and measured results for the case: three-element filtenna; f_0 = 4.8 GHz; FBW_s = 10 % and S_{11} < –10 dB

	f_0 [GHz]	$FBW_{-3\,dB}$ [%]	S_{11} @ f_0 [dB]	$FBW_{-10\,dB}$ [%]	S_{21} suppression [dB]	S_{21} selectivity [dB/GHz]	Maximal deviation [°]
Simulation	4.81	13.50	–9.37	–	–19.44	64.47	4.90
Measurement	4.84	16.52	–7.73	–	–19.85	66.45	5.99

The second test case of the three-element filtering array (f_0 = 5.8 GHz; FBW_s = 13 %; S_{11} < –15 dB) was manufactured and measured. The comparison of the simulated and measured responses of the S_{11} and the normalized realized gain are given in Figure 7.3 (left). The frequency response of the main lobe direction is shown in Figure 7.3 (right).

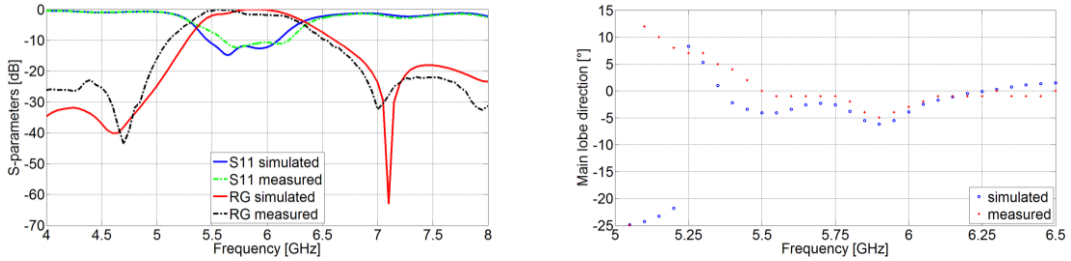

Figure 7.3 Comparison of the simulated and measured frequency responses of reflection coefficient and normalized realized gain (left) and main lobe direction (right) for the case: three-element filtenna; f_0 = 5.8 GHz; FBW_s = 13 %; S_{11} < –15 dB

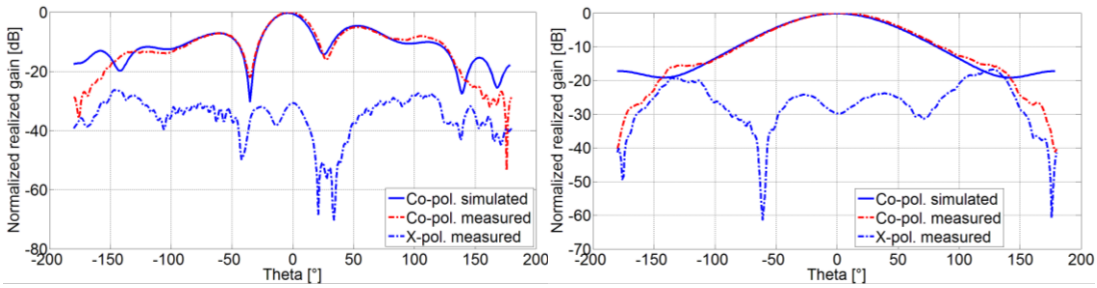

Figure 7.4 Comparison of simulated and measured co and cross polarizations in E-plane (left) and H-plane (right) of the three-element filtenna at frequency 5.8 GHz

The simulated co-polarization and cross-polarization components in the E-plane and the H-plane are confronted with measured ones in Figure 7.4. The realized gain of the filtering antenna array is about 9 dBi over the operating range. The important values are listed in Table 7.2. In this case, the results are in a good agreement.

Table 7.2 Comparison of the most important simulated and measured results for the case: three-element filtenna; f_0 = 5.8 GHz; FBW_s = 13 % and S_{11} < –15 dB

	f_0 [GHz]	$FBW_{-3\,dB}$ [%]	S_{11} @ f_0 [dB]	$FBW_{-10\,dB}$ [%]	S_{21} suppression [dB]	S_{21} selectivity [dB/GHz]	Maximal deviation [°]
Simulation	5.86	14.00	–11.88	11.02	–18.01	51.13	6.20
Measurement	5.77	14.89	–11.85	10.01	–21.92	49.68	4.99

The last test case of the three-element filtenna (f_0 = 6.8 GHz; FBW_s = 10 %; S_{11} < –10 dB) was manufactured and measured. The comparison of simulated and measured results of the S_{11}, S_{21RG} and the main lobe direction are depicted in Figure 7.5. The co-polarization and the cross-polarization components in the E-plane and in the H-

plane are shown in Figure 7.6. The maximal realized gain of the filtering antenna array is about 10 dBi. Figure 7.5 and Table 7.3 show that the results are in a good agreement.

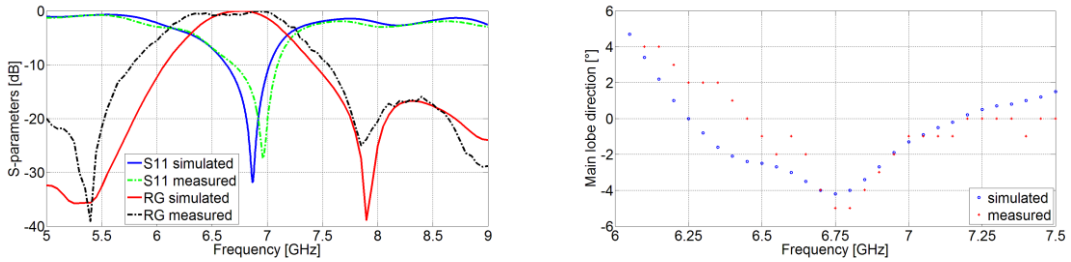

Figure 7.5 Comparison of the simulated and measured frequency responses of reflection coefficient and normalized realized gain (left) and main lobe direction (right) for the case: three-element filtenna; f_0 = 6.8 GHz; FBW_s = 10 %; S_{11} < –10 dB

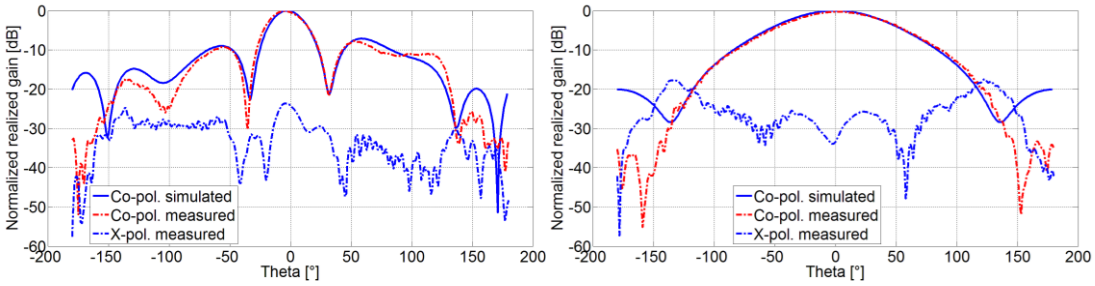

Figure 7.6 Comparison of simulated and measured co and cross polarizations in E-plane (left) and H-plane (right) of the three-element filtenna at frequency 6.8 GHz

Table 7.3 Comparison of the most important simulated and measured results for the case: three-element filtenna; f_0 = 6.8 GHz; FBW_s = 10 % and S_{11} < –10 dB

	f_0 [GHz]	$FBW_{-3\,dB}$ [%]	S_{11} @ f_0 [dB]	$FBW_{-10\,dB}$ [%]	S_{21} suppression [dB]	S_{21} selectivity [dB/GHz]	Maximal deviation [°]
Simulation	6.73	11.14	–18.67	5.74	–16.73	30.89	4.20
Measurement	6.64	16.11	–12.48	5.73	–15.95	32.27	4.99

The differences between simulated and measured results are given by the accuracy of manufacturing. Top and bottom layers of all three fabricated test cases of the three-element filtenna are shown in Figure 7.7.

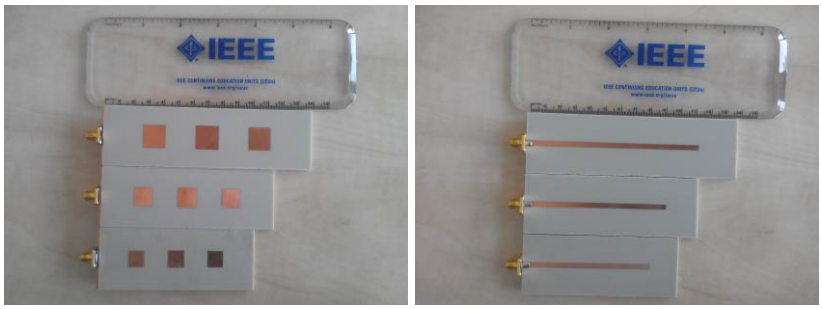

Figure 7.7 Top (left) and bottom (right) layers of the manufactured test cases of the three-element filtennas: upper at 4.8 GHz; middle at 5.8 GHz and lower at 6.8 GHz

7.2 Verification of the four-element filtering antenna array

In this Section, simulated and measured results of the three test cases of the four-element filtering array are compared. The first test case (f_0 = 4.8 GHz; FBW_s = 8 %; S_{11} < –15 dB) was manufactured and measured.

The comparison of simulated frequency responses of the S_{11} and the normalized realized gain with measured ones is shown in Figure 7.8 (left). The frequency response of the main lobe direction was measured and compared as well (right part in Figure 7.8). The simulated and measured co-polarization and cross-polarization components in the E-plane and the H-plane are shown in Figure 7.9. The realized gain of the filtering antenna array over the operating range is about 11 dBi. The most important parameters are listed in Table 7.4. In this case, the results are in a good agreement.

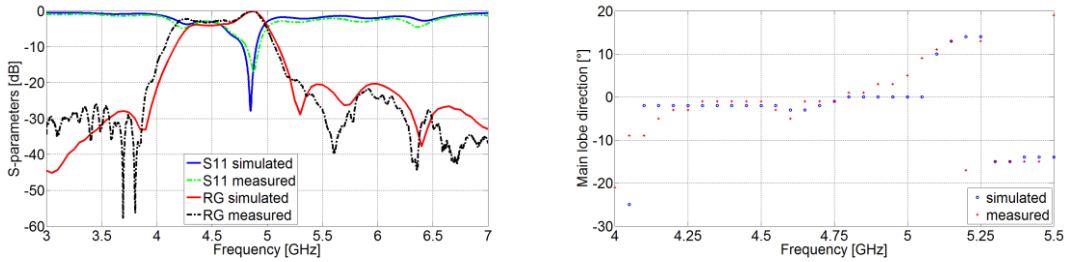

Figure 7.8 Comparison of the simulated and measured frequency responses of reflection coefficient and normalized realized gain (left) and main lobe direction (right) for the case: four-element filtenna; f_0 = 4.8 GHz; FBW_s = 8 %; S_{11} < –15 dB

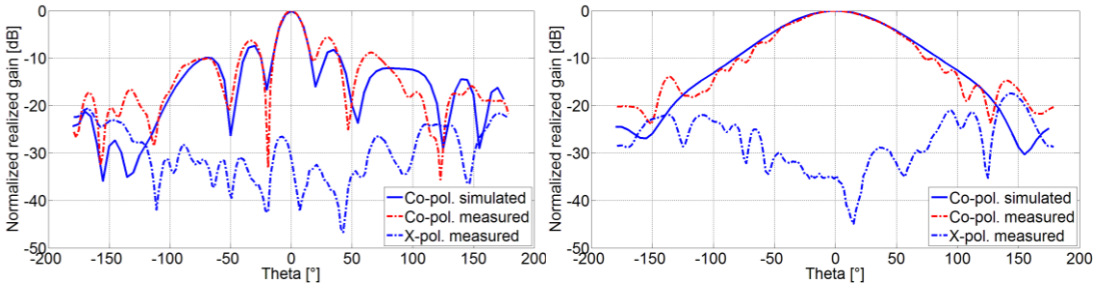

Figure 7.9 Comparison of simulated and measured co and cross polarizations in E-plane (left) and H-plane (right) of the four-element filtenna at frequency 4.8 GHz

Table 7.4 Comparison of the most important simulated and measured results for the case: four-element filtenna; f_0 = 4.8 GHz; FBW_s = 8 % and S_{11} < –15 dB

	f_0 [GHz]	$FBW_{-3\,dB}$ [%]	S_{11} @ f_0 [dB]	$FBW_{-10\,dB}$ [%]	S_{21} suppression [dB]	S_{21} selectivity [dB/GHz]	Maximal deviation [°]
Simulation	4.84	5.61	–21.53	2.67	–20.26	94.85	3.00
Measurement	4.82	5.89	–16.36	2.46	–21.69	76.16	5.00

The second test case of the four-element filtenna (f_0 = 5.8 GHz; FBW_s = 12 %; S_{11} < –10 dB) was manufactured and measured as well. Figure 7.10 (left) shows the comparison of measured frequency responses of the S_{11} and the normalized realized gain with simulated ones. The frequency dependencies of the main lobe direction over the operating range are shown in Figure 7.10 (right). The realized gain of the filtenna is about 11 dBi. The simulated and measured E-plane patterns and H-plane patterns of the

four-element filtenna at the frequency 5.8 GHz are illustrated by Figure 7.11. The global comparison is listed in Table 7.5. The results are in a good agreement.

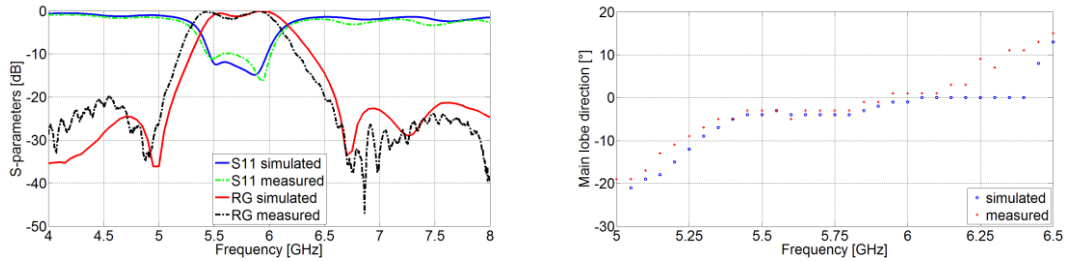

Figure 7.10 Comparison of the simulated and measured frequency responses of reflection coefficient and normalized realized gain (left) and main lobe direction (right) for the case: four-element filtenna; f_0 = 5.8 GHz; FBW_s = 12 % S_{11} < –10 dB

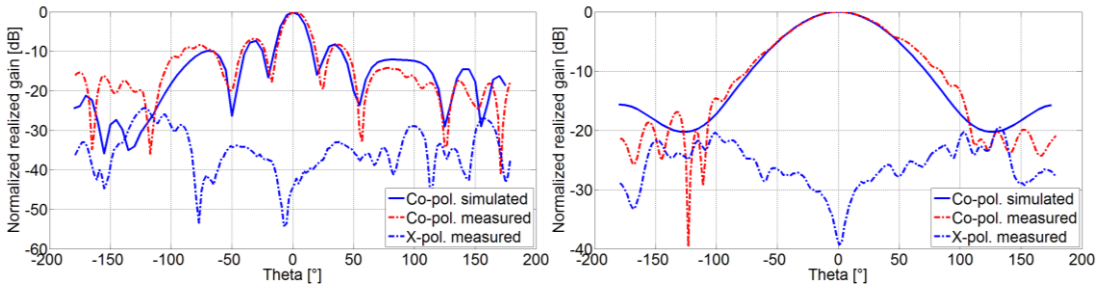

Figure 7.11 Comparison of simulated and measured co and cross polarizations in E-plane (left) and H-plane (right) of the four-element filtenna at frequency 5.8 GHz

Table 7.5 Comparison of the most important simulated and measured results for the case: four-element filtenna; f_0 = 5.8 GHz; FBW_s = 12 % and S_{11} < –10 dB

	f_0 [GHz]	$FBW_{-3\,dB}$ [%]	S_{11} @ f_0 [dB]	$FBW_{-10\,dB}$ [%]	S_{21} suppression [dB]	S_{21} selectivity [dB/GHz]	Maximal deviation [°]
Simulation	5.78	12.63	–13.77	9.24	–21.29	80.37	4.00
Measurement	5.68	13.52	–10.16	10.28	–19.76	75.33	5.00

The last test case of the four-element filtering array (f_0 = 6.8 GHz; FBW_s = 12 %; S_{11} < –20 dB) was manufactured and measured as well. The comparison of simulated and measured frequency responses of the reflection coefficient and the normalized realized gain are shown in Figure 7.12 (left). The frequency responses of the main lobe direction are illustrated in Figure 7.12 (right).

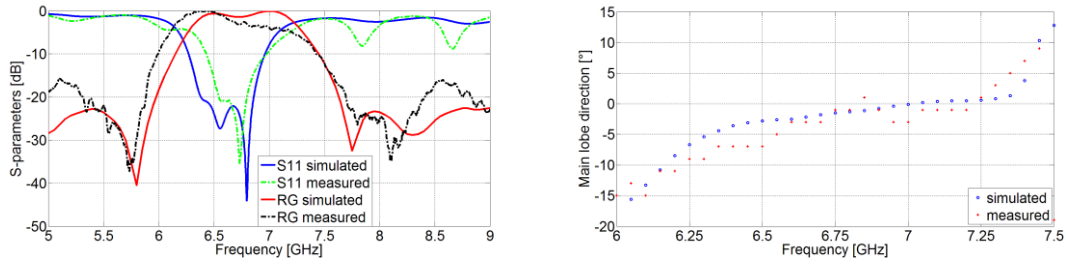

Figure 7.12 Comparison of the simulated and measured frequency responses of reflection coefficient and normalized realized gain (left) and main lobe direction (right) for the case: four-element filtenna; f_0 = 6.8 GHz; FBW_s = 12 %; S_{11} < –20 dB

This filtering array has a realized gain about 10 dBi. The simulated and measured E-plane patterns and the H-plane patterns of the four-element filtenna at the frequency 6.8 GHz are illustrated in Figure 7.13. The ripple losses in the pass band are equal to 1.4 dB. The most important parameters are listed in Table 7.6. Figure 7.12, Figure 7.13 and Table 7.6 show that the results are in a good agreement.

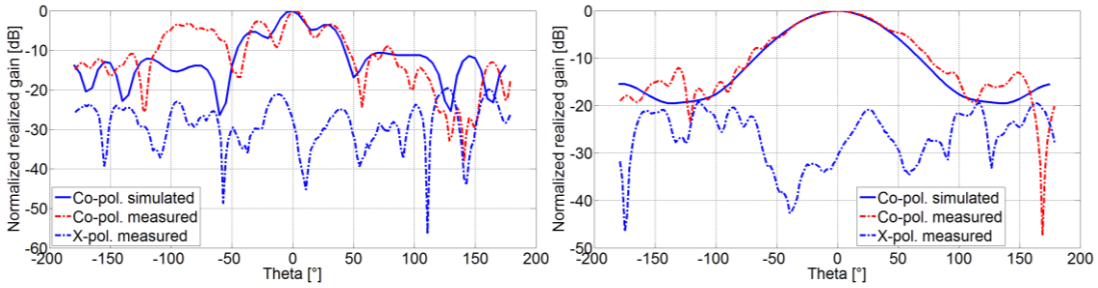

Figure 7.13 Comparison of simulated and measured co and cross polarizations in E-plane (left) and H-plane (right) of the four-element filtenna at the frequency 6.8 GHz

Table 7.6 Comparison of the most important simulated and measured results for the case: four-element filtenna; f_0 = 6.8 GHz; FBW_s = 12 % and S_{11} < –20 dB

	f_0 [GHz]	$FBW_{-3\,dB}$ [%]	S_{11} @ f_0 [dB]	$FBW_{-10\,dB}$ [%]	S_{21} suppression [dB]	S_{21} selectivity [dB/GHz]	Maximal deviation [°]
Simulation	6.76	13.13	–27.73	10.41	–22.76	82.23	5.40
Measurement	6.70	8.59	–25.01	8.06	–15.74	98.08	7.00

The differences between simulated and measured results are given by the manufacturing accuracy. Top and bottom layers of all three fabricated test cases of the four-element filtenna are shown in Figure 7.14.

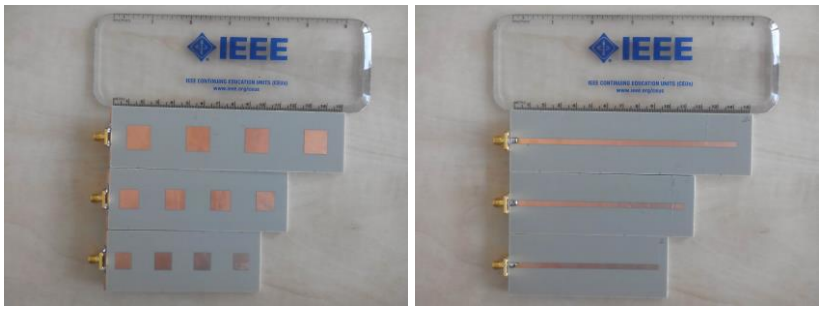

Figure 7.14 Top (left) and bottom (right) layers of manufactured test cases of the four-element filtennas: upper at 4.8 GHz; middle at 5.8 GHz and lower at 6.8 GHz

8 CONCLUSIONS

The dissertation thesis was focused on the numerical synthesis of filtering antennas. Attention was turned to the synthesis of the frequency responses of the S_{11}, the normalized realized gain and the main lobe direction of the antenna arrays fed by apertures. The antenna array fed by apertures was chosen since behaves like the filtering array without any filtering parts in the structure. The synthesis procedure was based on the equivalent circuit of the filtering antenna array and on the combination of the filter and the antenna approaches for its design. This process has not been published yet.

The "out-of-line" serial antenna array fed by apertures was chosen as an ideal compromise between all requirements as were:

- Final structure without any parasitic resonances.
- Direction of the main lobe does not dependent on the frequency, and is perpendicular to the structure over the operating range.
- The feeding network does not affect the radiation patterns.

Due to the used configuration of the structure, the antenna array exhibits only one main resonance without any parasitic one, and its main lobe is perpendicular to the substrate with maximal deviation 7°. Moreover, the frequency response of the normalized realized gain behaves like the output signal from the band-pass filter.

The width of the aperture (slot) W_s was a key parameter of the synthesis of the antenna array fed by apertures, and was included into the design procedure. We showed in the thesis that the width of the aperture has a dominant effect on the coupling between the patch antenna and the feeder (on the value of the *J*-inverter) and has a minor influence on the resonant frequency of the structure.

In the dissertation thesis, the main attention was focused on creation of the equivalent circuit of the filtenna. Second, we concentrated on the script in MATLAB which has sufficiently accurately approximated the results obtained from the full-wave model of the filtenna. Thanks to this approximation, we can save CPU time during the design of the filtering arrays.

The equivalent circuit consists from n parallel combinations of the *RLC*, which can simulate behavior of patch antennas, from n *J*-inverters, which can simulate the coupling between the patch antenna via the aperture to the feeder, and n+1 segments of the transmission lines, where the last segment represents an open end of the feeder (n is the order of the filtering antenna array).

The script in MATLAB is based on *ABCD* matrices of the transmission lines, the *RLC* combinations and the *J*-inverters. Results calculated by script in MATLAB, results simulated by the equivalent circuit in ANSYS Designer and results simulated by the full-wave model in CST Microwave Studio showed a very good agreement.

In the next step, the equivalent circuit was recalculated to obtain values of the low-pass prototype filter. The developed approach was compared again. All the results are equal, and due to this fact, the equivalent circuit can be used for the comprehensive synthesis of the filtering array which is based on the filter approach and g_i coefficients.

The comprehensive synthesis of the filtering antenna array fed by apertures is based on the combination of the filter design and the antenna design approaches. The filter design approach includes g_i coefficients, which were specially derived for the case of the three-element and the four-element filtering antenna array fed by apertures and calculation of the frequency response of the reflection coefficient (S_{11}). The antenna approach includes the calculation of the frequency response of the normalized realized gain which depends on the directivity D of the single patch antenna, on the array factor AF of the whole structure and the frequency response of the reflection coefficient S_{11} (on the values of the g_i coefficients). Due to g_i coefficients, the shape of the frequency responses of the reflection coefficient as well as the normalized realized gain could be altered and controlled.

The comprehensive synthesis of the filtering antenna array fed by apertures was verified on several test cases of the three-element filtenna and the four-element filtenna. In the first step, results calculated by script in MATLAB were confronted with the results obtained by the full-wave model in CST Microwave Studio. In the second step, three test cases of the three-element filtenna and three test cases of the four-element filtenna were manufactured, measured and compared with the results from full-wave model in CST Microwave Studio.

The verifications of the three-element filtennas were done over the frequency range from 4.8 GHz to 6.8 GHz, the fractional bandwidth of the whole structure varied from 7 % to 14 % and the acceptable level of the reflection coefficient was changed from –10 dB to –20 dB. The four-element filtennas were verified in the same frequency range and the same level of the S_{11}, only the fractional bandwidth of the whole structure was changed from 8 % to 12 %.

All test cases had only one resonant frequency. The maximal deviation of the main lobe was up to 7° over the operating frequency range, and the frequency responses of the normalized realized gain behave like the output signal of the band-pass filter with the selectivity between 30 dB/GHz and 66 dB/GHz in the case of the three-element filtenna, and between 75 dB/GHz and 98 dB/GHz in the case of the four-element filtenna.

This is the clear proof that the selectivity of the filtering antenna array depends on the order of the filtenna, and with growing order, the selectivity increases as well. Moreover, all confrontations of simulated and measured results were in a good agreement. These confrontations have clearly demonstrated the validity of the equivalent circuit, and the synthesis procedure used for the design of filtering antenna arrays. Small differences were caused by manufacturing inaccuracies.

This dissertation thesis brings a novel equivalent circuit of a filtenna, a novel formulation of g_i coefficients, and a novel procedure for the design of filtering antenna arrays. The developed synthesis procedure combines the frequency filter design and the antenna design. The synthesis gives accurate frequency responses of the reflection coefficient, the normalized realized gain and the main lobe direction. CPU-time demands of the developed synthesis procedure are in order of seconds in comparison with the full-wave computations which give results during several tens of minutes.

In future work, the presented filtering array can be generalized for higher orders. Also, tuning-space mapping can be used in combination with the presented equivalent circuit to improve the efficiency of the design.

REFERENCES

[1] YU, Ch., HONG, W. 37-38 GHz substrate integrated filtenna for wireless communication application. *Microwave and Optical Technology Letters*. 2012, vol. 54, issue 2, pp. 346-351. DOI: http://dx.doi.org/10.1002/mop.26589.

[2] YU, S., HONG, W., YU, Ch., TANG, H., CHEN, J. Integrated millimeter wave filtenna for Q-LINKPAN application. *2012 6th European Conference on Antennas and Propagation (EUCAP)*. DOI: http://dx.doi.org/10.1109/eucap.2012.6206170.

[3] YU, Ch., HONG, W., KUAI, Z., WANG, H. Ku-band linearly polarized omnidirectional planar filtenna. *IEEE Antennas and Wireless Propagation Letters*. vol. 11. DOI: http://dx.doi.org/10.1109/lawp.2012.2191259.

[4] TAWK, Y., COSTANTINE, J., CHRISTODOULOU, C. G. A varactor-based reconfigurable filtenna. *IEEE Antennas and Wireless Propagation Letters*. vol. 11. DOI: http://dx.doi.org/10.1109/lawp.2012.2204850.

[5] TAWK, Y., ZAMUDIO, M. E., COSTANTINE, J., CHRISTODOULOU, C. G. A cognitive radio reconfigurable "filtenna". *2012 6th European Conference on Antennas and Propagation (EUCAP)*. DOI: http://dx.doi.org/10.1109/eucap.2012.6206125.

[6] ZAMUDIO, M., TAWK, Y., COSTANTINE, J., KIM, J., CHRISTODOULOU, C.G. Integrated cognitive radio antenna using reconfigurable band pass filters. *Proceedings of the 5th European Conference on Antennas and Propagation (EUCAP)*, vol., no., pp.2108-2112, 11-15 April 2011.

[7] WOLANSKY, D., VSETULA, P., RAIDA, Z., HALL, P. S. Antennas with synthesized frequency dependency of gain. *2012 6th European Conference on Antennas and Propagation (EUCAP)*. 2012. DOI: 10.1109/eucap.2012.6206418.

[8] WU, W. J., YIN, Y. Z., ZUO, S. L., ZHANG, Z. Y., XIE, J. J. A new compact filter-antenna for modern wireless communication systems. *IEEE Antennas and Wireless Propagation Letters*. vol. 10. DOI: http://dx.doi.org/10.1109/lawp.2011.2171469.

[9] WU, W. J., WANG, J., FAN, R., ZHANG, Q. A broadband low profile microstrip filter-antenna with an omni-directional pattern. *Antennas and Propagation (APCAP), 2014 3rd Asia-Pacific Conference on* , vol., no., pp. 580–582, 26–29 July 2014 doi: 10.1109/APCAP.2014.6992560

[10] VERDU, J., PERRUISSEAU-CARRIER, J., COLLADO, C., MATEU, J., HUELTES, A. Microstrip patch antenna integration on a bandpass filter topology. *In proc. 12th Mediterranean Microwave Symposium (MMS2012)*, no. EPFL-CONF-179874. 2012.

[11] LIN, Ch.-K., CHUNG, S.-J. A compact filtering microstrip antenna with quasi-elliptic broadside antenna gain response. *IEEE Antennas and Wireless Propagation Letters*. vol. 10. DOI: http://dx.doi.org/10.1109/lawp.2011.2147750.

[12] LIN, Ch.-K., CHUNG, S.-J. A filtering microstrip antenna array. *IEEE Transactions on Microwave Theory and Techniques*. 2006, vol. 59, issue 11, s. 487-515. DOI: http://dx.doi.org/10.1142/9781848164543_0017.

[13] CHUNG, S.-J., WANG, H.-N. Compact multi-function antennas designed using filter synthesis technique. *2012 42nd European Microwave Conference (EuMC)*, vol., no., pp.1331-1334, Oct. 29 2012-Nov. 1 2012

[14] CHUANG, Ch.-T., CHUNG, S.-J. New printed filtering antenna with selectivity enhancement. *European Microwave Conference (EuMC 2009)*, vol., no., pp.747-750, Sept. 29 2009-Oct. 1 2009.

[15] CHUANG, Ch.-T., CHUNG, S.-J. A new compact filtering antenna using defected ground resonator. 2010 *Asia-Pacific Microwave Conference Proceedings (APMC), 2010* vol., no., pp.1003-1006, 7-10 Dec. 2010.

[16] CHUANG, Ch.-T., CHUNG, S.-J. A compact printed filtering antenna using a ground-intruded coupled line resonator. *IEEE Transactions on Antennas and Propagation*. vol. 59, issue 10, pp. 3630-3637. DOI: http://dx.doi.org/10.1109/tap.2011.2163777.

[17] LIN, Ch.-K., CHUNG, S.-J. A compact simple structured filtering antenna utilizing filter synthesis technique. *2010 Asia-Pacific Microwave Conference Proceedings (APMC)*, vol., no., pp.1573,1576, 7-10 Dec. 2010

[18] CHUANG, Ch.-T., CHUNG, S.-J. Synthesis and design of a new printed filtering antenna. *IEEE Transactions on Antennas and Propagation*, vol.59, no.3, pp.1036-1042, March 2011.

[19] KUFA, M., RAIDA, Z. Lowpass filter with reduced fractal defected ground structure. *Electronics Letters*. 2013, vol. 49, issue 3, pp. 199-201.
DOI: 10.1049/el.2012.3473.

[20] KUFA, M., RAIDA, Z. Comparison of planar fractal filters on defected ground substrate. *Radioengineering*, vol. 21, no. 4, pp. 1019-1024, December 2012.

[21] KUFA, M. *Planar fractal filters on defected ground substrate*. Diploma thesis. Brno University of technology, 2012.

[22] KUFA, M., RAIDA, Z. Design of filtenna with fractal defected ground structure. *European Conference on Antennas and Propagation (EuCAP), 2013 7th* , vol., no., pp. 1278-1280, 8-12 April 2013.

[23] VSETULA, P. *Antenna arrays with synthesized frequency response of gain.* Doctoral thesis. Brno University of Technology, 2014.

[24] VSETULA, P., RAIDA, Z. Dipole antenna array with synthesized frequency dependency of gain and reflection coefficient. *2013 International Conference on Electromagnetics in Advanced Applications (ICEAA)*. 2013.
DOI: 10.1109/iceaa.2013.6632410.

[25] BALANIS, C. A. *Modern antenna handbook*. Hoboken, NJ: Wiley, c2008, xviii, 1680 p. ISBN 04-700-3634-6.

[26] BALANIS, C. A. *Antenna theory: analysis and design*. 3rd ed. Hoboken: Wiley-Interscience, 2005, xvii, 1117 s. ISBN 978-0-471-66782-7.

[27] MILLIGAN, T. A. *Modern antenna design*. Hoboken: IEEE Press; John Wiley, 2005, xvi, 614 s. ISBN 04-714-5776-0.

[28] GARG, R. *Microstrip antenna design handbook*. Boston: Artech House, 2001, 845 s. ISBN 08-900-6513-6.

[29] CHRISTODOULOU, Ch. G., WAHID., P. F. *Fundamentals of antennas: concepts and applications*. Bellingham, Wash.: SPIE Press, 2001, x, 93 p. ISBN 08-194-4112-0.

[30] BANCROFT, R. *Microstrip and printed antenna design*. Atlanta, GA: Noble Publishing, 2004, p. cm. ISBN 18-849-3258-4.

[31] HONG, J. S., LANCASTER, M. *Microstrip filters for RF/microwave applications*. New York: John Wiley, 2001. ISBN 04-713-8877-7.

[32] POZAR, D. M. *Microwave engineering, 3rd ed*. Hoboken: John Wiley, 2005. ISBN 978-0-471-44878-5.

[33] CHEN, Wai-Kai. *The electrical engineering handbook*. Boston: Elsevier Academic Press, 2005, xviii, 1208 p. ISBN 01-217-0960-4.

[34] JARRY, P., BENEAT, J. *Advanced design techniques and realizations of microwave and RF filters*. Hoboken, N.J.: IEEE Press, c2008. ISBN 04-701-8310-1.

[35] JARRY, P., BENEAT, J. *Design and realizations of miniaturized fractal RF and microwave filters*. Hoboken, N.J.: Wiley, c2009, xiv, 194 p. ISBN 04-704-8781-X.

[36] HARISH, A., SACHIDANANDA, M. *Antennas and wave propagation*. New York: Oxford University Press, 2007, xviii, 402 p. ISBN 978-019-5686-661.

[37] POZAR, D. M., SCHAUBERT, D. H. *Microstrip antennas: the analysis and design of microstrip antennas and arrays*. New York: Institute of Electrical and Electronics Engineers, 1995, x, 431 s. ISBN 07-803-1078-0.

[38] WIRTH, W.-D. *Radar techniques using array antennas*. xvii, 470 pages. ISBN 978-085-2967-980.

[39] KUFA, M., RAIDA, Z., MATEU, J. Equivalent circuits of planar filtering antennas fed by apertures. *Microwaves, Radar, and Wireless Communication (MIKON), 2014 20th International Conference on* , vol., no., pp.1,4, 16-18 June 2014
doi: 10.1109/MIKON.2014.6899977

[40] KUFA, M., RAIDA, Z., VSETULA, P., WOLANSKY, D. Filtering antennas: Comparison of different concepts. *Antennas and Propagation in Wireless Communications (APWC), 2014 IEEE-APS Topical Conference on* , vol., no., pp.438,441, 3-9 Aug. 2014
doi: 10.1109/APWC.2014.6905565

CURRICULUM VITAE

Name:	Martin Kufa
Born:	The 4th of March 1988 in Chlumec nad Cidlinou, Czech Republic
Contact:	martinkufa11@gmail.com

Education:

2012 – 2015	Brno University of Technology Faculty of Electrical Engineering and Communication
Program title:	Electrical Engineering and Communication
Branch:	Electronics and Communication
Doctoral thesis:	Numerical Synthesis of Filtering Antennas
2010–2012	Brno University of Technology Faculty of Electrical Engineering and Communication
Program title:	Electrical, Electronic, Communication and Control Technology
Branch:	Electronics and Communication
Master thesis:	Planar Fractal Filter on Defected Ground Substrate
2007–2010	Brno University of Technology Faculty of Electrical Engineering and Communication
Program title:	Electrical, Electronic, Communication and Control Technology
Branch:	Electronics and Communication
Bachelor thesis:	Tunable ARC Frequency Filter
2003–2007	The Secondary School of Electrical Engineering Pardubice, Karla IV. 13

Languages: Czech, English

Specialization: Analysis and design of the antennas and the filters, modelling and simulation of the microwave structures and antenna measurement.

ABSTRACT

The dissertation thesis is focused on a complete design methodology of a three and four-element patch antenna arrays which are without any filtering parts and yet behave like a filtering antenna (filtenna). This design combines filter and antenna approaches and includes shaping the frequency response of the reflection coefficient and the modelling of the frequency response of the normalized realized gain. The frequency response of the main lobe direction is controlled as well. In order to control the shape of these responses, a set of g_i coefficients for designing the filtering antenna array are obtained. The design methodology was verified on the three and four-element filtennas over the frequency range from 4.8 GHz to 6.8 GHz; for fractional bandwidths from 7 % to 14 % and for levels of the reflection coefficient from –10 dB to –20 dB. The whole design methodology was supported by manufacturing and measuring six testing samples of the filtering antenna array with different configurations. Simulated and measured results show good agreement in all cases.